Journal of African Earth Sciences 160 (2019) 103605

Contents lists available at ScienceDirect

Journal of African Earth Sciences

journal homepage: www.elsevier.com/locate/jafrearsci

Sedimentary and paleobiological records of the latest Pleistocene-Holocene climate evolution in the Kordofan region, Sudan

Ahmed Dawelbeit[a], Etienne Jaillard[b,*], Ali Eisawi[c]

[a] Department of Geology, Faculty of Science, University of Kordofan, El Obeid, Sudan
[b] Université Grenoble Alpes, ISTerre, IRD, CNRS, IFSTTAR, CS 40700, 38048, Grenoble Cedex 9, France
[c] Al Neelain University, Faculty of Petroleum and Minerals, P.O. Box 12702, 11121, Khartoum, Sudan

ARTICLE INFO

Keywords:
Quaternary
Sedimentary environment
Paleobiological indicators
Paleoclimate
African humid period
Aeolian deposits

ABSTRACT

The study of the Quaternary sediments of the Kordofan region, Sudan, allowed to decipher the succession of environments in this area, since about 13 kyr. The oldest sediments (> 13 to 10.5 kyr BP) are mainly aeolian deposits, except in the southern areas. The "African Humid Period" is recorded by scattered palustrine and lacustrine carbonates dated at 10.5–6.5 kyr BP in the center and North, respectively, by fluvial deposits in the South, and by the pedogenesis of previous deposits in all areas. Fluvial activity may be responsible for the erosion of the previous aeolian sands in the southern areas. Between 6.5 and 3.3 kyr BP, the evolution from aquatic to terrestrial gastropod fauna, and from tropical to arid pollen assemblages points to the shift toward an arid climate. This aridification phase culminated between 3.3 and 1.1 kyr BP, with a period of strong aeolian activity and erosion. Aeolian deposition resumed after 1.1 kyr BP under conditions comparable to those of today. This evolution is consistent with that recorded in Saharan areas, although the period of strong aeolian erosion (≈3.3–1.1 kyr BP) may have been underestimated so far.

1. Introduction

The environmental evolution of Africa during the Late Quaternary has been studied for a long time, and unraveled a contrasted and highly variable evolution (e.g. Gasse, 2000; Nicoll, 2004; Williams, 2014, Gasse et al., 2008, and references therein). The present-day climate change enhanced the interest for climatic studies, which focused on past climate changes, their causes, forcing parameters, manifestations and consequences. In Africa, many of these studies have been carried out through detailed, multi-proxy and multidisciplinary analyses of cores drilled in lakes, paleolakes, deltas and offshore sediments, which constitute reliable, detailed and presumably continuous records of the environmental conditions that prevailed during deposition (e.g. deMenocal et al., 2000; Lézine et al., 2011; Collins et al., 2013; Costa et al., 2014; Revel et al., 2015; Bastian et al., 2017). In Central Sudan, other works focused on the White Nile Valley, its climatic and the hydrological evolution (Williams et al., 2000, 2006; 2015; Woodward et al., 2007; Barrows et al., 2014) and the related human settlements (Nicoll, 2004; Kuper and Kröpelin, 2006; Salvatori et al., 2011; Manning and Timpson, 2014; Gatto and Zerboni, 2015). However, the hydrological regime of the White Nile River is mainly controlled by climatic conditions prevailing at equatorial latitudes. Few studies addressed the analysis of sediments on a regional scale, which, in spite of less detailed records, may give a reliable paleogeographic image of the environmental and climatic evolution, and highlights the spatial and temporal variations of the sedimentary record (e.g. Servant, 1970; Pachur and Kröpelin, 1987; Hoelzmann et al., 2010).

On the other hand, geological studies in Sudan usually focused on mineral, hydrocarbon or groundwater resources, and overlooked Quaternary deposits. For the purpose of surficial water harvesting, Quaternary sediments are frequently excavated to form temporary pond for drinking water. Besides, these surficial deposits constitute the main surficial ground water reservoir, which may allow recharge of deeper groundwater reservoirs. For all these reasons, we undertook a regional study of the Quaternary deposits of the Kordofan region, in order to determine the main sedimentary facies and their environmental meaning, to specify their spatial distribution and to retrieve the information allowing us to reconstruct the environmental and climatic evolution of the study area.

* Corresponding author.
E-mail addresses: ahmeddawelbeit69@gmail.com (A. Dawelbeit), etienne.jaillard@univ-grenoble-alpes.fr (E. Jaillard), a.eisawi@neelain.edu.sd (A. Eisawi).

https://doi.org/10.1016/j.jafrearsci.2019.103605
Received 13 March 2019; Received in revised form 21 August 2019; Accepted 22 August 2019
Available online 27 August 2019
1464-343X/

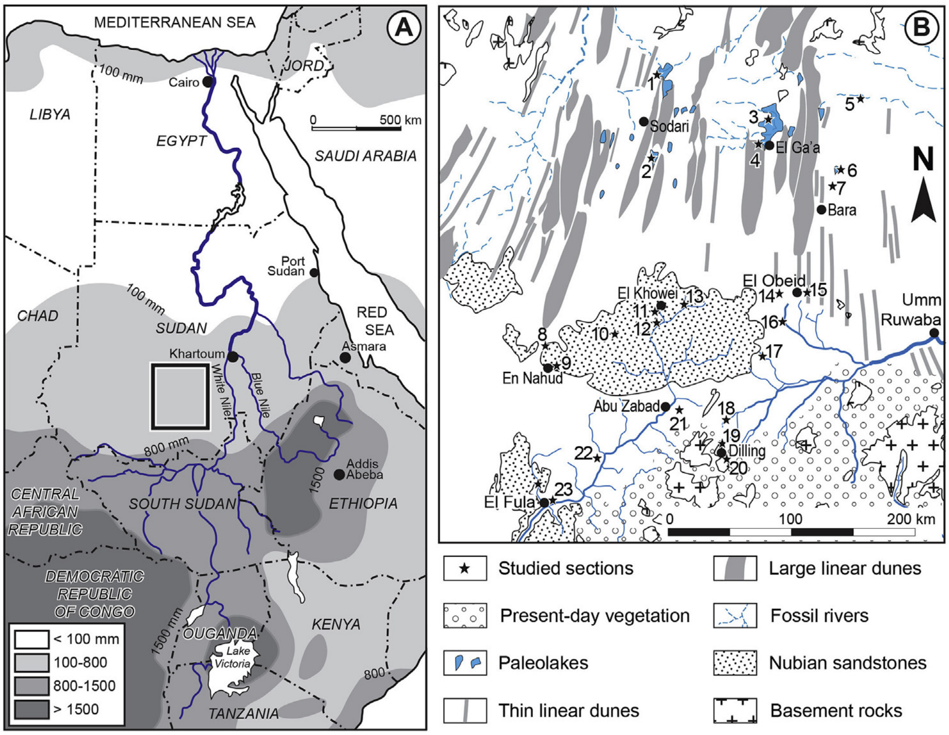

Fig. 1. Climate and location of the study area. A. Mean annual precipitations in Northeast Africa and location of the study area. B. Main geological and geomorphological features of the study area, and location of the main studied sites and sections. 1: North Sodari; 2: South Sodari, 3: North El Ga'a; 4: El Ga'a; 5: North Bara 3; 6: North Bara 2; 7: North Bara 1; 8. North En Nahud; 9. En Nahud; 10: West El Khowei; 11: El Khowei; 12: South El Khowei; 13: East El Khowei; 14: West El Obeid; 15: El Obeid; 16: South El Obeid 1; 17: South El Obeid 2; 18: South El Obeid 3; 19: North Dilling; 20: Dilling; 21: East Abu Zabad; 22: Um Dibeiba; 23: El Fula. Sites 1 to 7 define the northern area; sites 8 to 16 belong to the central area; sites 17 to 22 define the southern area.

2. Location and previous studies

2.1. Study area

The study area is situated in central-southern Sudan, in the Kordofan Region, West of the White Nile valley and SW of Khartoum. It is bounded by longitudes 28°00′ and 30°40′E, and latitudes 11°30′ and 15°00′N and covers an area of about 100.000 km^2 (Fig. 1).

The northern part of the study area is characterized by a low lying, gently undulating surface with few scattered, little elevated but sharp inselbergs (Fig. 2). This terrain is covered by extensive sand sheets, and N–S orientated sand dunes and stabilized sand dunes, forming dams crosscutting the ancient, fossil rivers. The relief of the central part is dominated by smooth V-shaped valleys (El Khowei-En Nahud), while to the East, the relief is marked by wide wadies. The southern part is characterized by steep massifs and inselbergs made of basement rocks, some of which are as high as 1300 m above sea level (Nuba Mountains). It is marked by a well-developed drainage pattern (Figs. 1 and 2) due to more abundant rainfalls and to clayey soils. Small wadies of this southern part flow either eastward, or southward toward the White Nile.

Nowadays, the annual rainfalls in the Kordofan region varies from less than 100 mm/year in the north (16°N), to more than 800 mm/year in the South of Southern Kordofan (10°S). In the study area, rainfalls vary from less than 200 mm/year to the North (Sodari, 14°30′N) to about 600 mm/year to the South (Dilling, 12°N) (Salih et al., 2018, Fig. 1A). Its central part (En Nahud, El Khowei, El Obeid) receives about 400 mm/year. The study area, therefore, belongs to the Sahel region (mean precipitations > 100 mm/year). The rainy season occurs in boreal summer, when the meteorological equator and the Inter-Tropical

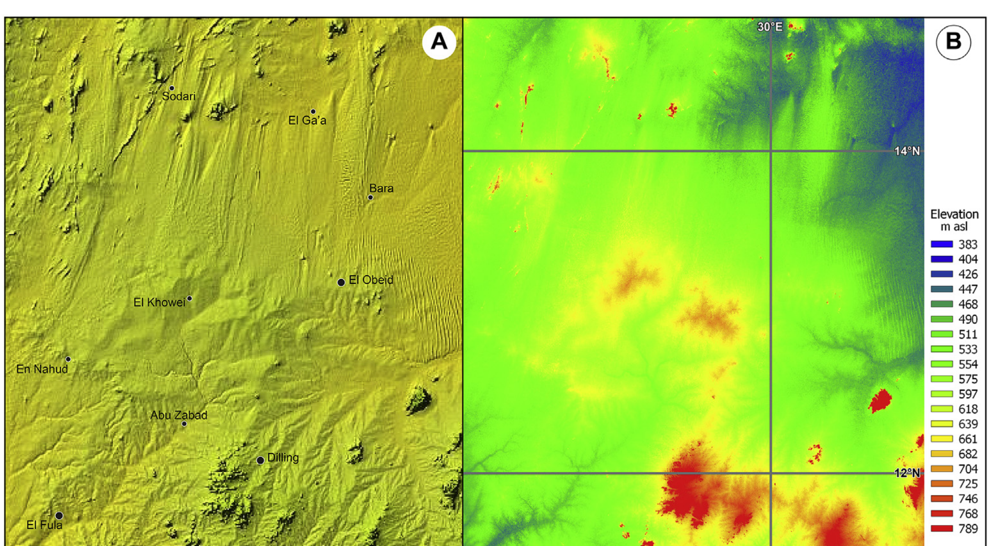

Fig. 2. Topography of the study area. A. Shaded image. B. Digital Elevation Model.

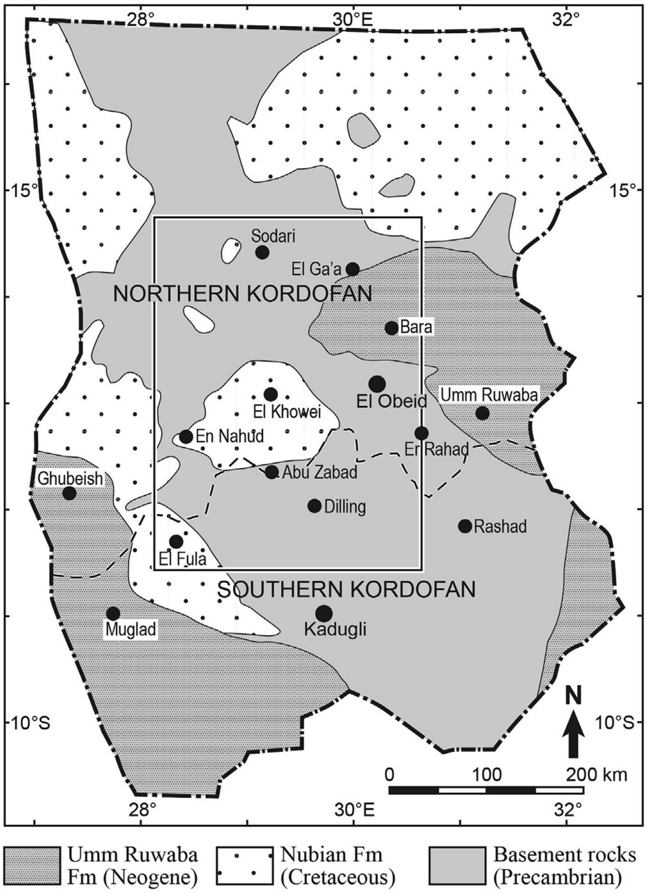

Fig. 3. Geological sketch of the Kordofan Province (from Rodis et al., 1968).

Convergence Zone (ITCZ) shift northward to the Tropic of Cancer, and the Congo Air Boundary impinges toward Southern Sudan and Ethiopia (Tierney et al., 2011). The mean annual air temperature is 27 °C, and temperature extremes of 10 °C and 46 °C are common to most areas. Monthly average temperatures fluctuate between 40 °C in summer and 22 °C in winter.

2.2. Geology

Rodis et al. (1968), and Whiteman (1971) and Vail (1978) provided good overviews of the geology of Kordofan and Sudan, respectively. According to these authors, the study area comprises a very discontinuous rock record spanning Precambrian rocks to recent deposits (Fig. 3). Basement rocks include high-grade to low-grade metamorphic rocks, crosscut by late-orogenic to post-orogenic granites and acid volcanic rocks. These are locally overlain by sandstone, shales and thin beds of limestone ascribed to the Paleozoic-Mesozoic. Most important is the widespread Nubian Sandstone or Nubian Group (Gp), which consists of conglomerates, sandstone and mudstone, deposited in continental to nearshore environments. They are usually ascribed to the Cretaceous (e.g. Schrank, 1994). The Nubian Gp represents one of the largest aquifer in the world, which extends through large parts of Sudan, Egypt, Libya and Chad (Voss and Solima, 2014).

The Nubian Gp then experienced a long period of *in situ* weathering under tropical climate marked by alternating wet and dry seasons. This led to the formation of highly ferruginous ferricrete (hematite and goethite), iron concretions and kaolinite-rich layers prior to mid-Miocene times (Rodis et al., 1968; Schwarz, 1994). The subsequent Umm Ruwaba Formation (Fm) consists mostly of mudstone, sandstone and conglomerates of lacustrine and fluvial environment (Fig. 3). The Umm Ruwaba Fm rests unconformably on basement rocks, or on the Nubian Gp, and is late Miocene to Pleistocene in age (El Shafie et al., 2011). In the northern part of Kordofan, recent deposits consist of widespread unconsolidated aeolian sand, stabilized dunes and residual soils, and redeposited fine material, known as the "Kordofan sand" and ascribed to the Quaternary (Edmond, 1942; Rodis et al., 1968; Warren, 1970; Whiteman, 1971). The latter has been ascribed to the Umm Ruwaba Fm by Vail (1978). In the southern part of the region, alluvium and slope-wash deposits are known in the valleys, while laminated, loosely compacted clay, silt and sand represent flood plain deposits (Rodis et al., 1968; Ruxton and Berry, 1978; Gunn, 1982).

2.3. Paleoclimate

In Northern Africa, the last interglacial episode (≈130–115 ka BP; Gierz et al., 2017) was a rainy period (Revel et al., 2010; Barrows et al., 2014; Tierney et al., 2017), while the Last Glacial Maximum (LGM) was marked by quite arid conditions and temperatures cooler than today (Gasse, 2000; Williams et al., 2006; Gasse et al., 2008). This period extended between 20 and 15 kyr BP and is documented as a period of dune building in the central Sahara, the Nile basin and East Africa (Nicholson and Flohn, 1980; Williams et al., 2000; Swezey, 2001; Woodward et al., 2007; Tierney et al., 2011; Williams, 2009, 2014). This hyper arid phase greatly influenced the geomorphology and landscape of the Saharan and surrounding regions.

This arid period is followed between ≈15 and 6 ka BP by a humid phase known as the "African Humid Period" (AHP) (deMenocal et al., 2000; Gasse, 2000; Drake et al., 2011; Williams, 2014; Gatto and Zerboni, 2015; Tierney et al., 2017). In the present-day Sahara, the AHP was characterized by the presence of numerous lakes and a savanna vegetation (Servant, 1970; Nicholson and Flohn, 1980; Szabo et al., 1995; deMenocal et al., 2000; Cole et al., 2009). In Sudan, these are the West Nubian Palaeolake (Pachur and Hoelzmann, 1991; Abell and Hoelzmann, 2000; Hoelzmann et al., 2010), the Selima lake (Haynes, 1982), and those formed along the Wadi Howar (Pachur and Kröpelin, 1987; Kröpelin and Soulié-Märche, 1991) and the Wadi Mansurab (Williams, 2009; Williams et al., 2015). In Sahara, some lake basins were exceptionally large, such as the Fezzan (Libya), Chad, or Chotts (Algeria) "megalakes" (Drake and Bristow, 2006).

During the late Holocene period (from 6 kyr BP onwards), the Sahara and Sahel regions recorded progressively drier condition (Lézine, 2009; Tierney and deMenocal, 2013; Manning and Timpson, 2014; Shanahan et al., 2015). This aridification period is well documented by the progressive drying of northern Chad (Kröpelin et al., 2008) and of the Sudanese paleo-lakes (Pachur and Kröpelin, 1987; Hoelzmann et al., 2010), by the gradual shift from moist to arid pollen assemblages in Lake Yoa (Chad; Lézine et al., 2011), or by the desertification (Bubenzer et al., 2007) and aeolian deflation recorded in the Middle and Late Holocene in Egypt and northern Sudan (Swezey, 2001; Nicoll, 2004).

2.4. Objective and methods

The present study is focused on the Quaternary sedimentary evolution of Central Kordofan and its environmental and climatic meaning, through the nature of the deposits, their paleontological and archeological content, and their lateral and vertical evolution. The main objectives of this study are thus (1) to determine the age, areal extent and lateral variations of the Quaternary sedimentary units of the study area, (2) to understand the processes that controlled the deposition and distribution of these deposits, and (3) to reconstruct the Quaternary environmental and climatic evolution of the Kordofan region.

Studied sections were selected according to their accessibility, the good exposure of thick and representative sedimentary successions, their organic matter content suitable for palynological analysis and radiocarbon dating, and the presence of gastropods for paleontological and paleobiological studies. The selected sites included river banks, road cuts, active or abandoned quarries and few hand-dug wells, providing 3 to 7 m-thick successions.

Sedimentological analysis have been carried out in the field with observations of the lithology, geometry of beds, nature of contacts and sedimentary features. The gastropods shells and their ecological habitat have been identified with the help of Dr Dirk Vandamme (Ghent University, Belgium). The analysis of pollen assemblages was carried out using standard palynological preparation techniques in the Petroleum Laboratories Research and Studies, Khartoum, by Mr Abdelbasit Mustafa and Miss Malaz Mohammed Ali. Vertebrate bones and archeological remnants were determined by Christophe Griggo from the Université Savoie Mont-Blanc (Chambéry, France) and Howeida M. Adam from the Archeology Department of the University of Khartoum (Sudan), respectively.

Radiocarbon dating have been performed in part by Dr. Tomasz Goslar from the Poznań Radiocarbon Laboratory, Poland, and for another part, by Dr. Jean Pascal Dumoulin from the Laboratoire des Sciences du Climat et de l'Environnement (LSCE), in Gif sur Yvette, France. Radiocarbon ages have been then calibrated using the Calib 14C calibration program, version 7.10 (http://calib.org/calib/calib.html) (Stuiver et al., 2019). These calibrated ages are quoted here as cal yr BP (Before Present).

2.5. Sedimentology

Seven sedimentary facies have been defined in the uppermost Quaternary deposits of the study area, which will be used to reconstruct the sedimentary evolution of the studied area.

2.6. Channelized conglomerate and coarse sand

Description: Channelized conglomerates may contain various types of lithoclasts: metamorphic rocks or quartz in areas floored by Precambrian rocks, iron concretions in areas close to the Nubian Gp, or calcareous nodules in many parts. In the first case, clasts are poorly sorted and angular in shape. In the other cases, nodules are little eroded and their shape is preserved. The base of the conglomerate beds is mostly an undulated surface, which separates the conglomerate from the underlying sediments or rocks (Fig. 4A). The thickest beds of conglomerates (up to 3 m thick) are found in the southernmost part of the study area. Lens-shaped coarse sand is formed of poorly sorted sand, exhibiting some small lithoclasts within the size-range of fine gravel. Its color varies from pale grey to reddish brown. This facies is marked by trough cross bedding and planar cross bedding (Fig. 4B). It usually occurs in lenses intercalated with other facies.

Interpretation: The angular shape and little erosion of the lithoclasts suggest that they underwent short transport. This is supported by the close relationship between the nature of the substrate and lithology of the clasts. The conglomerate beds or lenses suggest a strong fluvial activity. The occurrence of high-energy features and the erosional base of the conglomerate beds support the interpretation of deposition in high-energy fluvial channels. The poor sorting of the coarse sand, their lens shape and the occurrence of cross bedding indicate a high-to medium-energy fluvial deposition.

The calcareous concretions in conglomerates (Dilling area) are interpreted as reworked from previously deposited units containing these concretions. Channelized conglomerates in the southern part of the study area are made almost exclusively of iron concretions. The latter are regarded as re-deposited from the Nubian Gp, which crops out in the same area, and to the North in the El Khowei area (Fig. 23).

2.7. Alternating sand and silt

Description: This facies is formed of fine-to medium-grained sand, alternating with sandy shale and fine-grained sand beds (Fig. 4C). Cross bedding, current ripples and planar lamination are observed in the sand beds, which are locally poorly sorted or may present a fining-upward evolution (Fig. 4D). Laminae are mostly 2–5 mm thick, but may be 5 mm to 2 cm thick. The color of sand beds is red to reddish brown, while that of silt or shale beds varies from dark grey to green, and from reddish-brown to yellowish. The contacts between sand and silt levels are abrupt and conformable. In the southern area, these contacts may be erosional.

Interpretation: The occurrence of planar lamination and current ripples in the sand beds supports a moderate-to low-energy fluvial depositional environment (Boggs, 2006; Hewaidy et al., 2018). The alternation of sand and silt beds is assumed to be formed in the flood plain of a river. When the river comes out of its channel, it first deposits the coarse-grained sediments in a high-energy regime, and as the flood decreases in intensity, fine particles are laid down in a low-energy regime (Boggs, 2006). The locally observed fining upward evolution in sand beds indicates a gradual decrease in current strength through time, and supports the flood plain interpretation. The lens shape of some sand beds may represent crevasse splay deposits.

2.8. Mottled sand

Description: The mottled sand facies is characterized by coarse to very fine sand, presenting mottling, root traces and a noticeable organic matter content (Fig. 4E and F). Its color varies from green to reddish brown, and from grey to pale yellow. It may contain numerous calcareous concretions that vary in shape (Fig. 4G). The latter are usually scattered in the sand but may be concentrated in beds (Fig. 4H). Fine grained mottled sands prevail in the southern part of the area, whereas coarser grained facies dominate in the northern area.

Interpretation: Mottling or marmorization (Freytet and Verrecchia, 2002) in soil occurs when the iron content of sediments is > 2% and when water table fluctuations occur, thus favoring the migration of ferrous iron, which fixes as ferric iron (Ciolkosz and Dobos, 1990). The result is a mottled sediment with purple to yellow patches where ferric iron accumulated, and yellow or white stains in the area depleted in iron. Manganese and calcium can also migrate with iron, resulting in a complex fabric of mottled grey patches and ferruginous or calcareous concretions. As a consequence, the mottling facies indicates that the area experienced wet conditions under low oxidation rates (Freytet and Verrecchia, 2002).

The preservation of organic matter in soils and sediments mostly depends on its water content. Fine-textured soils hold nutrients and water, favoring plant growth. On the other hand, in wet soils, little oxygen is available for organic matter to decay, and organic matter can accumulate (e.g., Tóth et al., 2007; Schmidt et al., 2011). Therefore, the presence of organic matter in mottled sand facies suggests a humid climate, especially those marked by green to dark grey colors, while the mottled facies marked by pale grey, yellow and reddish colors may have experienced dryer condition and thus, oxidation.

Two forms of calcareous concretions or calcretes have been observed in the study area. The nodular calcretes are the most abundant and widespread, whereas tubular calcretes are restricted to some sites. Nodular calcretes may contain locally iron concretions (Fig. 4G) and quartz grains but are devoid of biogenic features. This points to a groundwater origin (Alonso-Zarza et al., 2011), related to shallow aquifer systems (Alonso-Zarza, 2003). The precipitation of carbonate occurs within a previous host rock and around the groundwater table (Alonso-Zarza, 2003).

Tubular calcretes (Chen et al., 2002; root calcretes of Freytet et al., 1997) are marked by an elongated shape and are concentrated in specific zones (lower part of Fig. 4H). Their typical morphology indicates that they formed by replacement of the root organic matter by calcium carbonate (Alonso-Zarza et al., 2011). The presence of biogenic features in the tubular calcretes indicates that they are formed in the vadose zone (Arakel, 1996), where precipitation of carbonate takes place mostly above the water table and within the sediment (Alonso-Zarza,

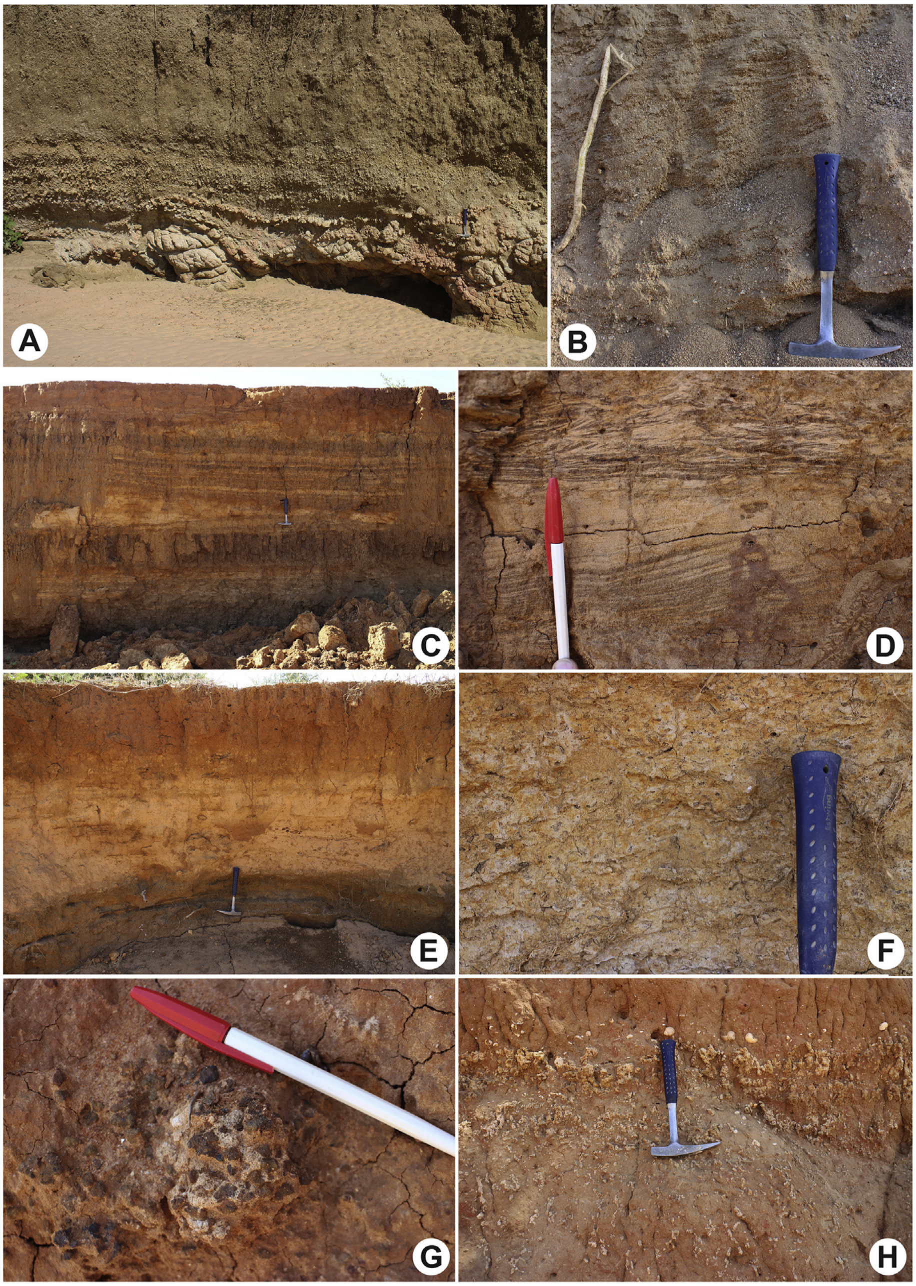

Fig. 4. Representative photographs of facies interpreted as subaerial deposits. A. Erosional contact of conglomerates on basement rocks, North Dilling. B. Trough cross-bedded coarse sand, Dilling. C. Alternating silt and sand, alluvial plain facies, South El Obeid 1. Dark layers are made of argillaceous silts corresponding to swamp deposits. D. Medium scale cross bedding and current ripples in a fluvial sand, South El Obeid 1. E. Transition between mainly fluvial, laminated sand facies and aeolian, red sand facies (top), South El Obeid 3. F. Mottled sand, East El Obeid. G. Calcareous nodule enclosing iron concretions, the latter being redeposited from the Nubian Gp, East Abu Zabad. H. Concentration of nodular calcareous concretions overlaying tubular concretions (roots), top of mottled sand facies, East El Khowei. Note the concentration of gastropod shells at the base of the overlying red sand facies. (For interpretation of the references to color in this figure legend, the reader is referred to the Web version of this article.)

2003). Difference in concretion size could also be due to additional reprecipitated carbonate, since the latter tends to concentrate near the surface and within the voids (Chen et al., 2002). Together with the occurrence of root molds, tubular calcretes indicate a significant vegetation cover.

2.9. Red sand facies

Description: The red sand facies is dominated by fine grains, but coarser sands are locally found in the northernmost part of the study area. The sand is usually quite well sorted, homogeneous and devoid of any current features (Fig. 4E, upper part). The sediment looks cemented; the red color is common in all parts, but reddish brown colors are found locally.

Interpretation: The usual absence of sedimentary features, the good sorting and the prevailing fine grains suggest that these structureless, loess-like sediments were laid down by aeolian processes (Collinson, 1986; Glennie, 1987). However, in the southern areas, some fine-to medium-grained intercalations of fluviatile sands suggest that the aeolian deposits were sporadically re-deposited and sorted by alluvial processes. The hardness of the sediment and its reddish color is probably due to its cementation with iron oxide. Edmond (1942) reported that they are typical wind deposited sand with well-rounded quartz grains and a color varying from pale buff to deep red, the red color being due to iron staining on the surface of the quartz grains.

2.10. Sandy carbonate facies

Description: This facies is formed of massive, poorly lithified limestone beds, locally sandy to silty (Fig. 5A). It is deeply karstified and presents root casts and molds (Fig. 5B), and frequent desiccation features. Well preserved gastropod shells are common, and may be concentrated either at the top of the bed, or within the bed itself. Sandy carbonate beds grade laterally to concentrations of nodular calcretes forming beds. This facies occurs locally as clasts re-deposited in subsequent deposits.

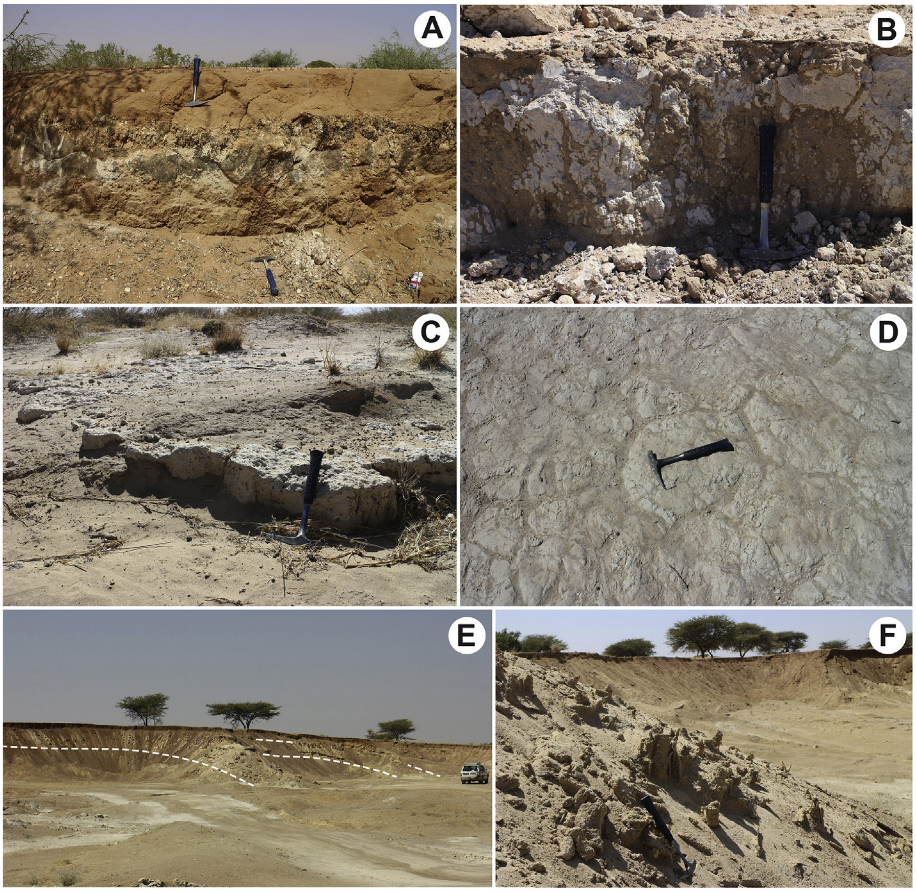

Fig. 5. Representative photographs of facies interpreted as subaqueous deposits. A. Sandy carbonate, overlain by the red sand facies, El Khowei. B. Karstified palustrine limestone showing also root traces, En Nahud. C. Lacustrine limestone showing numerous root traces, South of Sodari. D. Desiccation cracks in lacustrine limestone, North of Sodari. E. Clinoform-bearing coarse-grained, deltaic deposits, paleo-lake of El Ga'a. F. Tubular root traces in deltaic deposits, paleo-lake of El Ga'a. (For interpretation of the references to color in this figure legend, the reader is referred to the Web version of this article.)

Interpretation: The lithology and sedimentary features of this facies indicate a shallow, subaqueous deposition, frequently exposed to desiccation. It is consequently interpreted as a palustrine deposit (Freytet and Verrecchia, 2002; Alonso-Zarza, 2003; Alonso-Zarza et al., 2011). Pure or granular limestone is formed in the bottom of shallow water bodies, while silty to sandy limestone is formed in shallower water (Alonso-Zarza, 2003). However, soils accumulated in the lake shores are sometimes very rich in carbonates and are true palustrine limestones (Freytet and Verrecchia, 2002), which grade laterally to layers of nodular calcretes formed in clastic deposits within the vadose zone (Alonso-Zarza et al., 2011).

2.11. Carbonate and argillaceous sand facies

Description: This facies consists of 15–50 cm thick, marly or chalky calcareous beds (Fig. 5C), locally deeply karstified and brecciated in its upper part, or presenting desiccation cracks (Fig. 5D). It exhibits white to pale grey color, and is marked by the occurrence of abundant gastropod shells and locally, of ostracods. In the El Ga'a hand-dug well, three horizons of this facies have been observed, alternating with grey to yellowish argillaceous sands. The latter consists of fine-to medium-grained sand in a friable argillaceous matrix, locally containing irregular lacustrine limestone clasts, and is intercalated with the carbonate facies. Near Sodari, these calcareous beds are locally silicified.

Interpretation: The deposition of limestone requires the presence of a permanent water body. The scarcity of sandy component and the low density of the sediment, ascribed to the presence of abundant diatom frustules, suggest a deeper depositional depth. This facies is, therefore, interpreted as deposited in a lacustrine environment. The deeply karstified and brecciated upper surfaces of the limestone beds indicate subaerial exposure, which is common in lacustrine environment (Freytet and Verrecchia, 2002; Alonso-Zarza, 2003).

Lakes are dynamic systems sensitive to subtle changes in climate, such as fluctuations in precipitation and run-off, leading to alternating sedimentation features (Tucker and Wright, 1990). The existence of karst and breccia in the upper surface of the carbonate layers indicates that the lake has filled up and desiccated more than one time. Conversely, the intercalations of argillaceous sand suggest sporadic, abrupt increases of clastic supply, attributable to floods of the river flowing into the lake, leading to the deposition of distal deltaic deposits. The local occurrence of reworked limestone fragments in the latter supports an abrupt change in the energy regime (see below).

2.12. Steeply sloping coarse sand

Description: This facies has been only observed in a quarry located north of El Ga'a. It comprises coarse sand and gravel beds, the strata of which exhibit a marked inclination (Fig. 5E). The color varies between red in the upper part and pale yellow in the lower beds. It overlies the lacustrine limestone of the El Ga'a paleo-lake revealed by a hand-dug well. The thickness of these sediments exceeds 5 m in the quarry and decreases toward the East or Southeast, toward the paleo-lake. Some fine-grained beds exhibit well preserved gastropod shells and thick, tubular root molds (Fig. 5F).

Interpretation: The coarse material of this facies indicates the proximity of a river that supplied the clastic material. The well-marked sloping strata are interpreted as clinoforms and the fact that they overly lacustrine sediments imply deposition in a delta that prograded into the El Ga'a paleo-lake. This indicates that this area must have locally experienced a marked fluvial activity during the phase of lake forming. The presence of gastropod shells mostly living at the shoreline, suggests an intermittent regime of the river feeding the delta. The presence of thick root molds (Fig. 5F) indicates vegetation growing close to the shoreline. The argillaceous sand beds alternating with lacustrine

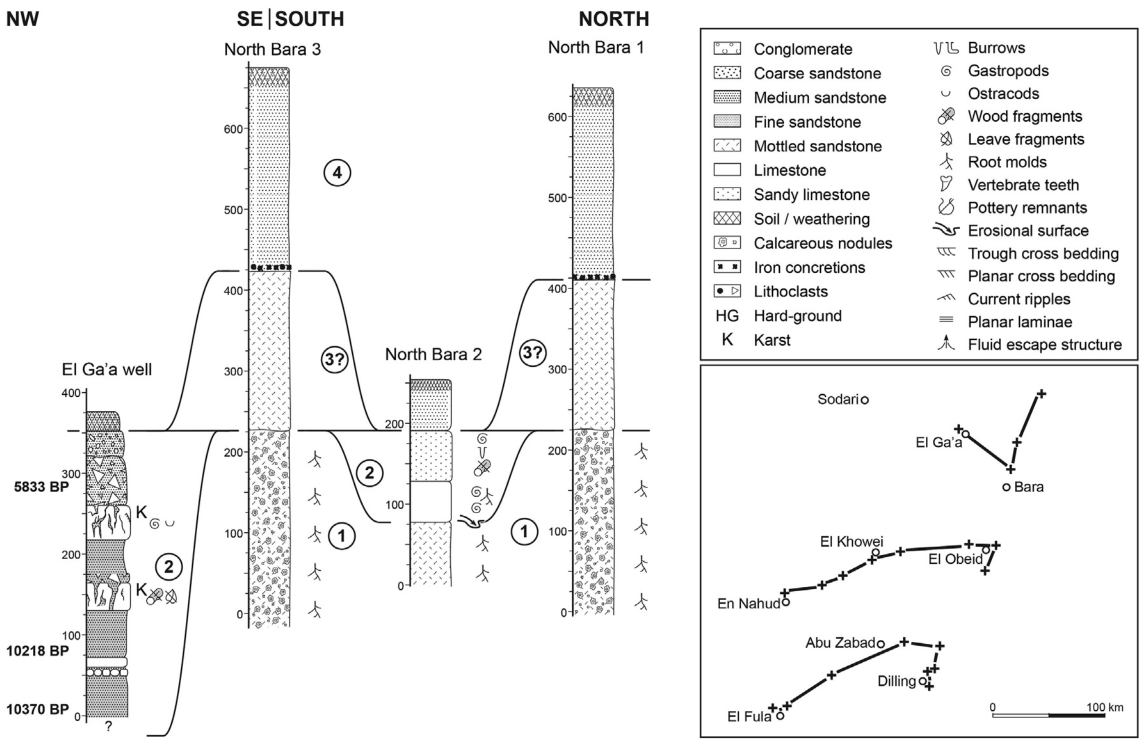

Fig. 6. Representative sections of the late Quaternary deposits in the northern part of the study area.

carbonates in El Ga'a (section IV.6; Fig. 6) are, therefore, interpreted as prodelta deposits.

2.13. Thin gravel horizon

Description: In the northern areas (Bara and farther north), the upper part of the succession is locally marked by a thin horizon of iron concretions and rock gravels, apparently interbedded within yellowish to reddish fine sand.

Interpretation: The presence of thin beds of coarse material interbedded within aeolian deposits suggests lag deposits left out by the wind activity. These layers are thus interpreted as overlying a deflation surface (Glennie, 1987; Durand and Bourquin, 2013).

3. Stratigraphy and archeology

3.1. Stratigraphy

The study of more than twenty sedimentary sections (Fig. 1B) reveals highly variable stratigraphic successions, according to the areas. Because of very rapid lateral facies variations in the late Quaternary succession of Kordofan, we distinguished four chronostratigraphic units, based mainly on discontinuities and radiocarbon dates (Table 1), and on a lesser extent on lithological properties and sedimentary facies. Because of still sparse radiocarbon dates, the stratigraphic scheme presented below must be considered provisional.

Unit 1 (U1) has been recognized in all areas except Dilling, and is the lowermost observed stratigraphic unit (Figs. 6 and 7). It is composed of mottled, variegated, fine-to coarse-grained sand containing numerous nodular calcretes. Where visible, this unit unconformably rests on the Nubian Gp (El Fula) or on basement rocks (Dilling, Abu Zabad). From organic matter disseminated in the sand, we obtained ^{14}C ages of 7779 ± 94 cal yr BP East of El Khowei, and 12 874 ± 168 cal yr BP East of Abu Zabad (Fig. 7). However, on one hand, the base of this unit has not been precisely dated, and on the other hand, organic matter is probably younger than the surrounding sand (see section VII.2). This lower unit is, therefore, ascribed to the latest Pleistocene (> 13 kyr BP) to 8 kyr BP interval.

Unit 2 (U2) is represented in the central zone by mottled sand and palustrine calcareous beds, by lacustrine limestone, argillaceous sand, and clinoform-bearing coarse clastic sand in the northern area, and by fluvial, cross-bedded, coarse sand and conglomerates in the southern part of the study area (Figs. 6 and 7). Its lower contact may be either gradual, or abrupt and conformable. In En Nahud, Williams (2009) mentions small lakes dated at 7650 ± 90 cal yr BP. Organic matter contained in limestone layers provided ^{14}C ages of 10 370 ± 124, 10 218 ± 38 and 5833 ± 83 cal yr BP in El Ga'a (Figs. 6), and 9720 ± 200 and 6352 ± 56 cal yr BP in En Nahud (Fig. 7). Since we collected the latter sample very close to the surface, the latter age may be result from partial contamination with present-day organic matter. Nevertheless, we consider the age of U2 comprised between ≈10.5 and 6.5 kyr BP.

Unit 3 (U3) is restricted to the eastern and southeastern part of the studied areas. It is made of mottled sand intercalated with few fluvial sand layers. The basal contact is conformable. East and South of El Obeid, charcoal and organic matter were dated at 3351 ± 95 and 3264 ± 95 cal yr BP (Fig. 7). North of Dilling, organic rich sandy shales (swamp deposits) yielded ^{14}C ages of 4526 ± 93 and 4067 ± 85 cal yr BP (Fig. 7). In North Dilling, a piece of charcoal in a conglomerate bed underlying U4 yielded an age of 7615 ± 184 cal yr BP (Fig. 7). Since the latter charcoal is probably reworked, this unit is ascribed to the ≈6500 to 3300 years BP interval, keeping in mind, however, that these stratigraphic units may be time-transgressive (see below).

Unit 4 (U4) crops out in all areas and is the uppermost stratigraphic unit. It is mainly made of fine-to medium-grained red sand (red sand facies). However, in the southwestern area (Dilling), it is locally made of fine-grained, homogenous brown sand, interbedded with sand beds of fluvial origin. Its lower limit is a locally strongly erosional surface. Carbonized wood and plant remains found in this unit yielded ^{14}C ages of 692 ± 34 and 596 ± 56 cal yr BP around Dilling, and 1021 ± 66 and 838 ± 79 cal yr BP south of El Obeid (Fig. 7). Therefore, this unit is considered younger than ≈1100 years BP.

Table 1
Radiocarbon (C^{14}) dates from samples of the study area. See Figs. 1B, 6 and 7 for location of samples.

Sample	Section	Depth	Laboratory	Material	Lab code	^{14}C age BP	Age	±
	(cm)	cal yr BP	(2σ)					
NDel 16-17	North Dilling 2	375	LSCE	paleosol	49 432	4055 ± 30	**4526**	93
NDel 16-18	North Dilling 2	337	–	paleosol	49 433	3720 ± 30	**4067**	85
NDel 16-20	North Dilling 2	135	–	paleosol	49 434	740 ± 30	**692**	34
NDel 16-2	North Dilling 1	250	–	charcoal	50 046	6750 ± 110	**7615**	184
Del 1-2	Dilling	40	Poznan	charcoal	Poz-79741	165 ± 30	modern	-
Del 2-1	Dilling	185	–	charcoal	Poz-79743	595 ± 30	**596**	56
Ga 6-1	El Ga'a	360	LSCE	paleosol	50 047	9195 ± 45	**10 370**	124
Ga 6-3	El Ga'a	290	–	paleosol	49 435	9040 ± 40	**10 218**	38
Ga 6-7	El Ga'a	85	–	paleosol	40 436	5095 ± 30	**5833**	83
Kh 1-1	South El Obeid 1	185	Poznan	charcoal	Poz-79737	910 ± 30	**838**	79
Kh 1-2	South El Obeid 1	280	–	charcoal	Poz-79739	1120 ± 30	**1021**	66
En Nahud	En Nahud	0	–	limestone	Poz-81611	5565 ± 35	**6352**	56
AWZ 1-4	En Nahud	0	–	limestone	Poz-91229	8680 ± 80	**9720**	200
Sonj 9	South El Obeid 3	340	LSCE	paleosol	49 437	3140 ± 30	**3351**	95
KT 1-1	East El Obeid	220	Poznan	paleosol	Poz-79736	3050 ± 35	**3264**	95
KT 4-2	East El Obeid	65	–	bone	Poz-0	–	not suitable	–
Ka 1-1	South El Obeid 3	30	–	charcoal	Poz-79740	132.9 ± 0.35	modern	–
Dod 1	East El Khowei	440	LSCE	paleosol	50 044	6960 ± 50	**7779**	94
Dab 1	East Abu Zabad	650	–	paleosol	50 045	10 960 ± 100	**12 874**	168
Ga 4-3a	El Ga'a	0	Poznan	bone	Poz-0	–	not suitable	–
Ga 4-3b	El Ga'a	0	–	bone	Poz-0	–	not suitable	–
Ga 4-3c	El Ga'a	0	–	bone	Poz-0	–	not suitable	–
Ga 5	El Ga'a	0	–	bone	Poz-93016	108.47 ± 0.36	modern	–
Sod 3-1	Sodari	0	–	bone	Poz-93017	107.86 ± 0.31	modern	–
S Sod 1-2	Sodari	0	–	bone	Poz-0	–	not suitable	–
S Sod 3	Sodari	0	–	bone	Poz-0	–	not suitable	–

This succession and the age data call for three important remarks. Firstly, the Quaternary surficial deposits of the Kordofan region are most probably of latest Pleistocene age, and mainly of Holocene age, the Holocene being defined as the period younger than 11 700 years BP (e.g. Lewis and Maslin, 2015). Second, U1 may be as young as 8 kyr BP, while U2 can be as old as 10 kyr BP. This indicates either that the boundary between lithological U1 and U2 is, at least locally, diachronous, depending on the local topography and/or depositional environment, or that some ^{14}C ages are erroneous, due to contamination by modern organic matter. Other lithological boundaries, therefore, may be also diachronous. Finally, the presently available data suggest that there was a hiatus between U3 and U4, i.e., between ≈3.3 and 1.1 kyr BP. This point is discussed below.

3.2. Archeology

Pottery fragments, chipped stones and grindstone have been found along a paleo-shore of the large paleo-lake located north of El Ga'a, i.e. probably in the upper part of Unit 2 (Fig. 8). The potteries include the dotted wavy lines decorative, banded decorative, polished and thin, and polished and thick. The banded and polished sherds are historic potteries (Merowetic and Islamic eras).

The dotted wavy line ornamentation has a wide distribution west of the Nile across the Sahara-Sahel belt (Haaland, 1992; Mohammed-Ali and Khabir, 2003; Sadig, 2010) and has been classified as Mesolithic. Reappraisal of the chronology of cultural development in central Sudan suggests that the Mesolithic period spans the ≈10 to 7 kyr BP interval (Salvatori and Usai, 2007; Salvatori et al., 2011, 2014). Therefore, the age suggested by potteries ornamented with dotted wavy lines is consistent with the ^{14}C dates (≈10.5–6.5 kyr BP) obtained from Unit 2.

3.3. Paleobiology

The habitat of fossil gastropods and the pollen assemblages have been taken as paleoenvironmental proxies. Poorly dated vertebrate bones could not be interpreted reliably.

3.4. Gastropods

Gastropods shells are observed in abundance in the central and northern parts of the study area, but mainly in Units 2 to 4 (Fig. 9). The species identified include aquatic, semi-aquatic and land snail species. Seven of them are aquatic freshwater snails: *Biomphalaria sudanica*, *Biomphalaria pfeifferi*, *Gabbiella senaariensis*, *Bulinus truncatus*, *Melanoides tuberculata* and *Radix natalensis*. The semi-aquatic species are *Pila wernei* and *Lanistes carinatus*, while land snail species are *Limicolaria flammea, Limicolaria caillaudi* and *Caracolus* sp. (Dawelbeit, 2018).

The stratigraphic distribution of the gastropod shells was documented in the En Nahud and East El Khowei 1 sections (Fig. 9), i.e. in the central part of the study area (Fig. 1). In both sites, the gastropod shells are concentrated in Units 2 and 4. Only the *in situ*, well-preserved gastropod shells were counted. 175 shells of four different species were counted in the En-Nahud section, and 739 shells of eleven species were counted in the east El Khowei section. The results indicate an absolute domination of the aquatic and semi-aquatic species in Unit 2, reflecting humid climatic conditions between ≈10.5 and 6 kyr BP. The lower part of Unit 4 is dominated by land snails, and locally by semi-aquatic and aquatic groups (Fig. 9). This distribution may indicate either a sub-humid to semi-arid environment between ≈1100 and ≈ 700 yr BP, or the re-deposition of some shells of aquatic snails at the base of Unit 4, after the hiatus observed between ≈3.3 and 1.1 kyr BP (see Fig. 4H). In both sections, the upper part of Unit 4 is totally dominated by land snail species (mainly *L. flammea*) (Fig. 9), which suggests that there were no longer permanent water bodies in this area during the last ≈1100 yr.

3.5. Palynology

Twenty-nine samples from six sites were analyzed for palynological studies. However, three sites were proved barren of pollens, and have been excluded from the results. The twenty-two analyzed samples from the North Dilling, South El Obeid 3 and South El Obeid 1 sections yielded a total of 1408 pollen and spores (831 in El Obeid 3, 399 in North Dilling and 178 in South El Obeid 1; Fig. 10). 1213 palynomorphs out of the total counted specimens have been classified into four main

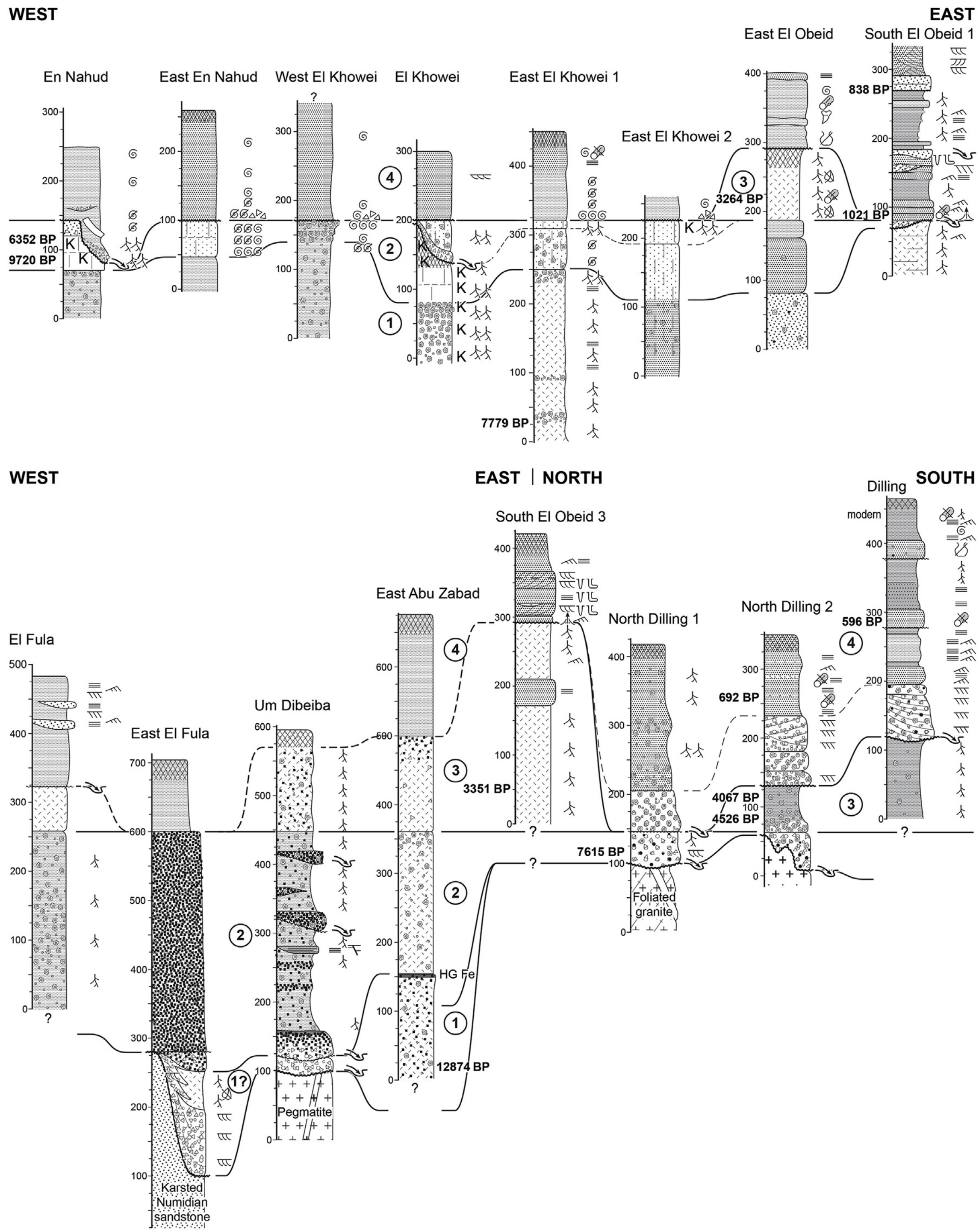

Fig. 7. Representative sections of the late Quaternary deposits in the central (above) and southern part (below) of the study area. Caption and location on Fig. 6.

groups, which are indicators of aquatic, tropical, savanna and arid environments (Table 1, Fig. 10).

Due to few dates in the studied sections, the exact chronology of the transition between the distinct palynomorphs assemblages is difficult to specify. Furthermore, all studied sections are located in the central and southern areas, and no data have been obtained from the northern part of the study area. However, all sections display a sharp decrease of palynomorphs indicative of aquatic and tropical environment around 1100 years BP, and a correlative increase of savanna and arid vegetation (Fig. 10). Although the occurrence of tropical or aquatic palynomorphs in fluvial deposits at the base of Unit 4 (South El Obeid 1, North Dilling) may be due to the depositional environment, the climate seems to have become comparable to that of today, by ≈ 900 years BP (Dawelbeit, 2018).

3.6. Bone fragments

Poorly preserved bone fragments have been found along the paleoshore of paleolakes located North of El Ga'a, and North and South of Sodari (Fig. 8). Unfortunately, they are too poorly preserved to be determined at a species or genus level, and they were either not suitable for ^{14}C dating (lack of collagen for five samples), or yielded very recent

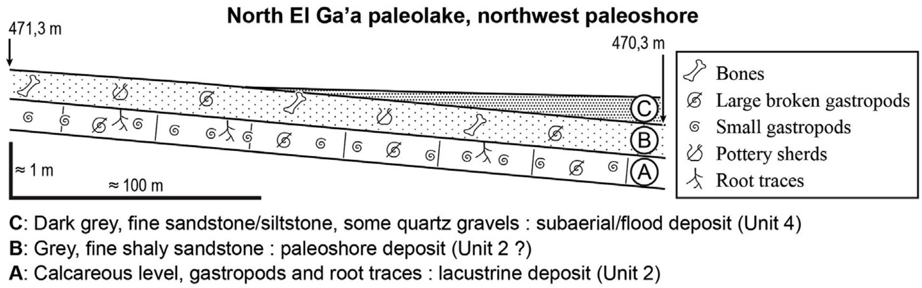

Fig. 8. Sketchy section of the outcrops yielding archeological and vertebrate remnants on the northwestern shore of the paleolake located North of El Ga'a (site 3 on Fig. 1B).

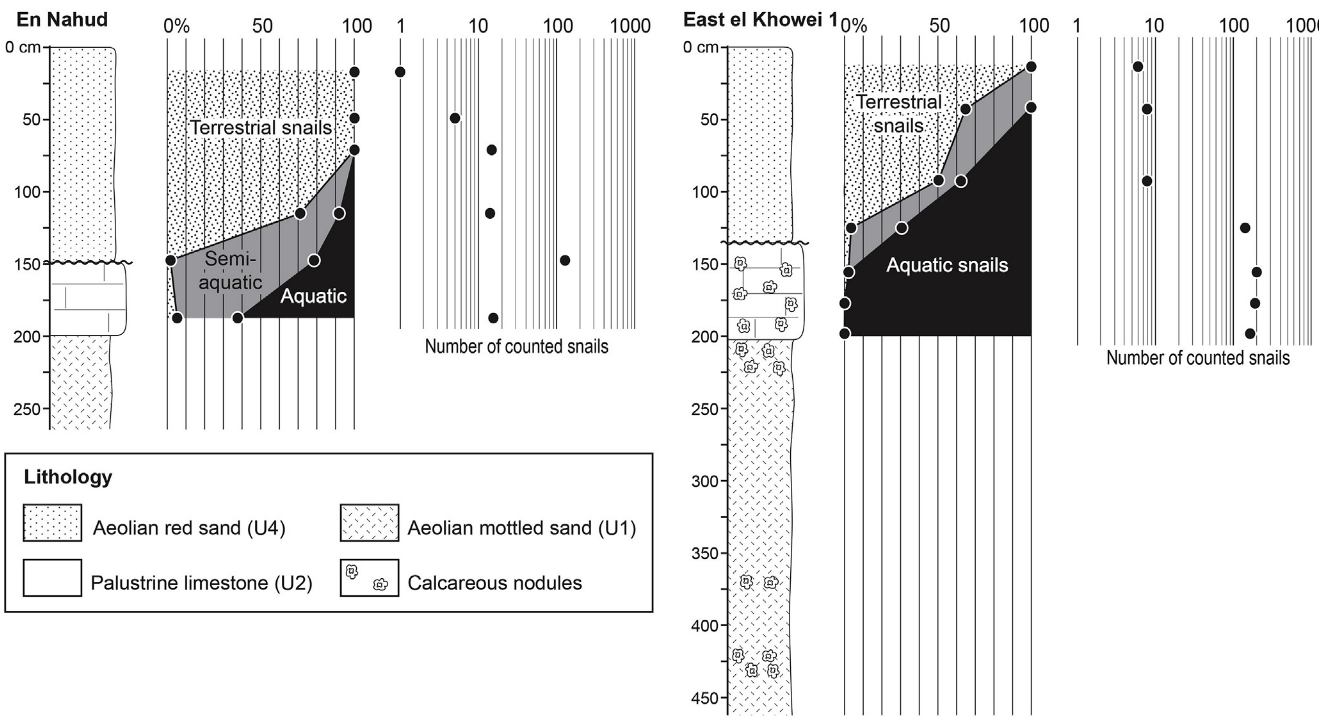

Fig. 9. Distribution and types of gastropods in the En Nahud and East El Khowei sections.

ages (108.47 ± 0.36 cal yr BP North of El Ga'a, and 107.86 ± 0.31 cal yr BP near Sodari; Table 1). Dr. Griggo identified numerous remnants of ox (scapula, calcaneus, tibia, talus), of other medium sized herbivores (metatarsal, coast, jaw), a possible radius of dromedary, and two tibias of undetermined, very large herbivores (El Ga'a). Because of the lack of reliable dates, and because some of them may proceed from Unit 4, no interpretation can be made about this vertebrate fauna.

3.7. Sedimentary and climatic evolution

The presented chronologic, sedimentary, paleobiological and archeological data allow us to reconstruct the sedimentary and climatic evolution of the studied area (Fig. 11).

3.8. 13 000–10 500 years BP period (U1)

This period is marked by the deposition, in most of the study area, of presently mottled, variegated, fine-to coarse-grained sand containing numerous nodular calcretes (U1). Since the mottled sands are aeolian deposit (Edmond, 1942; Dawelbeit, 2018), they suggest an arid climate during deposition. Mottling and calcrete formation are interpreted as due to subsequent pedogenesis.

The lack of deposition around Dilling, is interpreted as due to a more humid climate combined with a rough topography that favoured erosion and sediment transport by rivers during this period and the subsequent one (Fig. 11). This interpretation is supported by the abundance of coarse conglomerates in the southern areas (Fig. 7), which suggests that rivers were significantly more active in the southern areas than in the North at that time. Since very few fluvial deposits are observed in the northern area (Fig. 6), this suggest that a climatic gradient existed, as presently, between the northern areas dominated by aeolian processes, and the southern area that recorded heavier rainfalls responsible for significant fluvial activity.

3.9. 10 500–6 500 years BP period (U2)

This period is represented in the central zone by mottled sand and palustrine sandy limestone beds, by lacustrine limestone, argillaceous sand, and deltaic clinoform-bearing coarse clastic sand in the northern area, and by fluvial, cross-bedded, coarse sand and conglomerates in the southern part of the study area (Figs. 6, 7 and 11). Gastropods and tubular calcretes are frequent in the central area, while gastropods, ostracods and diatoms are common in the scattered lacustrine deposits in the North. These deposits evidence a humid climate, favoring the development of lakes and swamps in the North, and the activity of

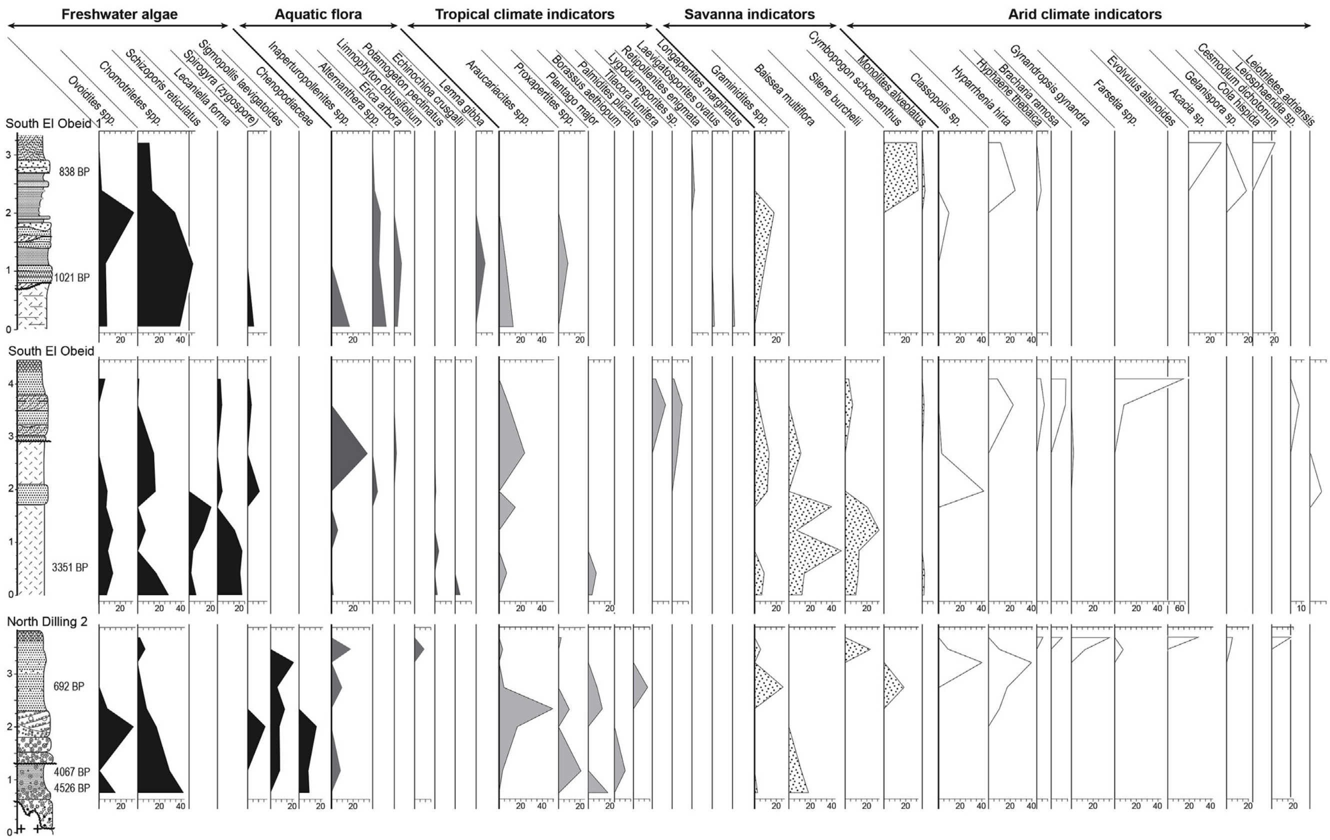

Fig. 10. Synthetic pollen diagrams of percentages *versus* depth, in the North Dilling 2 and South El Obeid 1 and 3 sections. Black areas: fresh water algae; Dark grey areas: aquatic flora; Light grey areas: tropical vegetation; Dotted areas: savanna vegetation; White areas; arid vegetation.

rivers in the South.

As a matter of fact, the aquatic gastropods-bearing palustrine deposits found on the plateau formed by the Nubian sandstone in the En Nahud – El Khowei area, cannot be fed by large rivers (see Fig. 2). Therefore, they were necessarily fed by direct rainfalls, the latter being responsible for the rise of the ground water table. Consequently, we propose that the pedogenesis of the formerly deposited aeolian sands (U1) occurred during this period, giving way to the development of mottling and nodular calcretes in Unit 1. In the Nile valley southwest of Khartoum, Dal Sasso et al. (2018) dated calcareous concretions between 11.5 and 6.1 kyr cal BP, which is consistent with our interpretation. This humid period might also be responsible for the lack or scarcity of pollens and gastropods in Unit 1 (Figs. 9 and 10), through oxidation and dissolution by seeping water. Lacustrine sediments are only known in the North, where they seem to be restricted to small depressions located along dry rivers dammed by large rectilinear dunes (El Ga'a, Sodari, Figs. 1B–2). Together with the presence of a delta in the El Ga'a lake (site 4 in Fig. 1B), this suggests that these lakes were fed by rivers draining large areas (Figs. 1B, 2 and 11). The finding of Mesolithic artifacts on the paleoshore of these lakes shows that the climatic

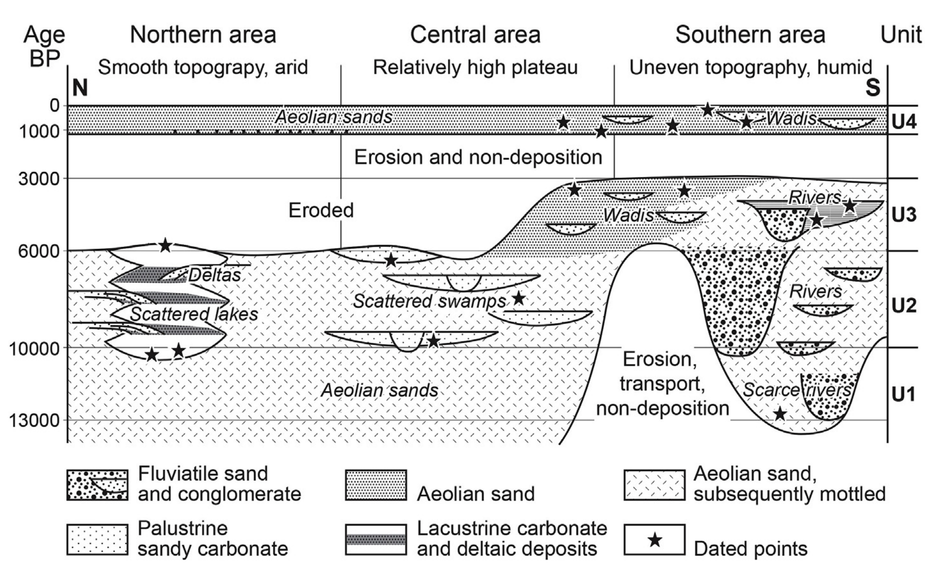

Fig. 11. Synthesis of the sedimentary and climatic evolution of the study area.

conditions were compatible with human settlements, at least close to the lake.

In the El Khowei – En Nahud area, the occurrence of mottled sand dated at ≈ 8000 years BP, underlying palustrine limestones (East El Khowei) and of palustrine carbonates dated at 10 500 to 6 500 years BP (En Nahud, El Ga'a) suggests that, either the swamps were not permanent or not present everywhere during this period, or the organic matter of some dated samples from Unit 2 had been contaminated by recent roots. In the former case, the boundaries between lithological units may not represent time lines. In the Dilling area, sedimentation seems to have begun later, maybe because of the activity of strong rivers that eroded and transported away all available sediment.

In most areas, except for lacustrine or fluviatile deposits, Unit 2 is rather thin (usually less than 1 m), although it encompasses a 4000–5000 years long period. This may be due to the lack of wind, or more probably, to the stabilization of the sand, because of a significant vegetation cover and to soil development.

3.10. 6500 - 3300 years BP period (U3)

Only the southern and eastern parts of the study area seems to have received deposits during this period (Figs. 6, 7 and 10). They consist of mottled sands intercalated with few fluvial laminated sand layers (East El Obeid, South El Obeid 3), interpreted as being deposited by aeolian processes (Dawelbeit, 2018). These sands subsequently and locally underwent pedogenesis and reworking (transportation, sorting and deposition) by fluvial activity, thus suggesting a still humid climate. North of Dilling, palustrine organic-rich, laminated grey sandy shale to clayey sands indicate local presence of ponds to the South between 4500 and 4000 years BP.

Meanwhile, the En Nahud-El Khowei area did not receive any sediments between 6000 and 1100 years BP, and the top of the palustrine limestone of U2 is sharply eroded. Since a deflation surface (Glennie, 1987; Durand and Bourquin, 2013), marked by a thin layer of iron concretions and gravels has been observed in the northern part of the study area (north of Bara; Fig. 6), this hiatus may be ascribed to a period of significant wind erosion (Fig. 11). Because the northern areas were more exposed to winds blowing from the Sahara, and the En Nahud – El Khowei area is a relatively high plateau, they may have experienced a stronger exposure to wind activity and erosion. In addition, deep erosion is clearly evidenced in the En Nahud-El Khowei area by the undulated erosional surface on top of the palustrine carbonates.

3.11. 3300 - 1100 years BP period (hiatus)

No deposits of that age are known in the study area. This period is marked either by the deflation surface observed in the northern part of the study area (Fig. 6), or by erosional surfaces capping the mottled sands around El Obeid, the palustrine deposits in the En Nahud - El Khowei area, and the flood plain sediments around Dilling (Fig. 7). This period is thus interpreted as a period of aeolian erosion and/or non-deposition in most of the study area (Fig. 11), although fluvial deposition may have locally continued in the southernmost part, where dates are scarce.

3.12. 1100 years BP to present (U4)

Deposition resumed 1100 year ago in the whole region with fine-to medium-grained red sand interpreted as loess-like aeolian deposits. The absence of pedogenetic processes in these sands in the northern part of the study area indicates that deposition took place under dry and windy condition. The pollen assemblages confirm this interpretation, since aquatic and tropical palynomorphs are rapidly replaced by savanna and arid pollen assemblages around 1100 years BP (Fig. 10). However, in the southern areas, U4 may present interbeds of flood plain deposits (El Fula) and is locally made of fine-grained brown sand, interbedded with sand beds (South El Obeid, Dilling), expressing the reworking and sorting out of the aeolian deposits by fluvial processes (Fig. 7).

This unit is thus interpreted as deposited in an arid environment, except in the southern area, where the activity of rivers indicates more humid conditions, as evidenced by current features, root molds, plant remnants, and the local development of calcareous concretions (Fig. 11). In contrast to Unit 2, Unit 4 may be more than 3 m thick, especially in the South (Fig. 7), thus expressing a high sedimentation rate. This may be explained both by a significant aeolian activity, in the absence of vegetation in the northern zone at that time, which made available significant amounts of sand. Moreover, the southern areas being a relative topographic depression (Fig. 2), aeolian deposition may have been favoured on the leeside of the more elevated central area.

3.13. Comparison with other areas and discussion

Because paleoenvironmental studies are scarce in the Sahelian area (Bristow and Armitage, 2016; Drake and Bristow, 2006; Lancaster et al., 2002; Schüster et al., 2005; Lézine et al., 2011), many comparisons have been made with the Saharan region.

In the study area, sediments deposited between 13 and 10 kyr BP are interpreted as aeolian deposits corresponding to an arid period, subsequently deeply transformed by pedogenesis. The 15–10 ka interval is known as a period of intense dune building and dune activation (Nicholson and Flohn, 1980; Swezey, 2001; Woodward et al., 2007). In Lake Chad basin, Servant and Servant-Vildary (1980) mention a period of wind activity between 20–18 and 13 kyr BP. In Mauritania, Lancaster et al. (2002) identified three dune generations of distinct orientations, dated at 25–15 ka, 12–10 ka and after 5 kyr BP, respectively, whereas Collins et al. (2013) noticed a strong aeolian dust influx between 18 and 12 kyr BP. In the Nile delta, multiple geochemical proxies indicate an arid period from 17.5 to 14.5 kyr BP (Castaneda et al., 2016).

The existence of a Holocene humid period in Sahara has been recognized for a long time (Servant, 1970; Pachur and Kröpelin, 1987; deMenocal et al., 2000; Gasse, 2000; Kuper and Kröpelin, 2006; Kröpelin et al., 2008; Lézine et al., 2011; Drake et al., 2011; Shanahan et al., 2015; Skonieczny et al., 2015). In the Nile delta, it is marked by mineralogical and geochemical evidences (Hamann et al., 2009; Castaneda et al., 2016; Bastian et al., 2017), and by a high sedimentation rate between 15 and 8 kyr BP (Blanchet et al., 2013; Revel et al., 2015). It would be due to the Northward shift of the intertropical rain belt, and to Eastward incursion of Congo Air masses (Costa et al., 2014). West of Khartoum, lakes and ponds have been dated between 9.9 and 7.6 cal kyr BP along Wadi Mansurab (Williams, 2009; Williams et al., 2015). In the same area, swamps periodically inundated by overflows from the White Nile River allowed human settlements between ≈10 and 8 kyr BP (Salvatori et al., 2011, 2014). One must keep in mind, however, that the hydrological regime of the White Nile River depends on climatic conditions prevailing more than 1000 km farther South.

The abrupt or progressive nature, and the exact age of the beginning and end of the “African Humid Period” are, however, still debated (deMenocal et al., 2000; Hoelzmann et al., 2004; Gasse et al., 2008; Tierney and deMenocal, 2013; Foerster et al., 2012; Shanahan et al., 2015; Gatto and Zerboni, 2015; Collins et al., 2017). Unfortunately, our dates are too sparse to allow us to specify this point. However, a striking feature of the study area is the contrasting depositional systems, marked in the southern and central areas, by noticeable fluvial activity and rain fed swamps, respectively, and in the northern areas by isolated lakes fed by rivers, located upstream of large dunes that dam fossil rivers.

The period from 6.5 to 4 kyr BP is widely acknowledged as a period of rapid increasing aridity in the Sahara and Sahel (e.g. Gasse, 2000; Nicoll, 2004; Shanahan et al., 2015). This time span records, however, local spells of humid climate, for example in Lake Chad around 5–4 ka (Servant, 1970; Schüster et al., 2005; Bristow and Armitage, 2016) or in

Nubia around 2.5 kyr BP (Nicoll, 2004). Arid to hyper arid conditions comparable to those of today are reached by 2 kyr BP.

The hiatus identified in Kordofan between 3.3 and 1 kyr BP, is interpreted as due to a strong wind activity, which precluded deposition in the whole area, and removed sediments deposited between 6 and 3 kyr BP in the northwestern parts of the study area. In the Saharan area, Gasse (2000) quoted a dry event at 4.5–4 kyr BP. In southern Egypt, as much as 30 m of sandy sediments were locally removed by wind erosion (Haynes, 1985; *in* Nicoll, 2004). This deflation period marked by erosional surfaces has been recognized in Nubia between 4.7 and 2.5 kyr BP (Nicoll, 2004), and in the Western Nubia paleolake at ≈ 4 ka BP (Pachur and Hoelzmann, 1991). Stokes et al. (2004) quoted an enhanced dune reactivation between 6 and 7 and 3 kyr BP in central and northern Mali. Farther West, a phase of dunes building is recorded after 5 kyr BP in Mauritania (Lancaster et al., 2002), and an increase of aeolian dust input has been detected offshore West Africa around 5–3 ka (Collins et al., 2013). In the Nile delta, a peak of aridity is recorded by an increase of Saharan dust and a very low contribution of Ethiopian particles between 4.5 and 3.7 kyr BP (Blanchet et al., 2013) and between 3.7 and 2.6 kyr BP (Revel et al., 2015), while Woodward et al. (2007) mentioned catastrophic low floods of the Nile river between 4.5 and 4.2 kyr BP. Therefore, the Late Holocene desertification phase seems to be associated, at least in Northeastern Africa, with a period of intense wind activity around 4.5 to 2.5 kyr BP (Swezey, 2001).

The hiatus identified in the study area may have begun during this 4.5 to 2.5 ka period. The significant erosion and/or the deflation surface recorded in the central and northwestern parts of the study area is ascribed to a stronger exposure to wind erosion, due to the northward sloping topography and the relatively high elevation (500–700 m asl). Conversely, the southern and eastern parts of the study area are located farther from the Saharan winds, from which they are sheltered by the elevated plateau formed by the En Nahud-El Khowei area (Fig. 2). Additionally, the wetter climate of the southern areas may have contributed to the more rapid pedogenesis and stabilization of the deposited aeolian sands of Unit 3, favoring its preservation.

From 1.1 kyr BP to present, the climate in Kordofan seems to have been comparable to the present-day climatic conditions. Recently, Zerboni and Nicoll (2019) suggested that herding activities enhanced soil erosion and dust generation in northeastern Africa since ≈ 7 kyr BP. Although our observations are too scarce to support this interpretation, this process may have contributed to the hiatus and erosion observed in the study area between 3.3 and 1 kyr BP.

The contrast observed during the Holocene between the northern areas dominated by aeolian sediments and scattered lakes or swamps, and the southern areas dominated by aeolian sands and fluvial deposits (Fig. 11) may be ascribed to the proximity of the Nuba Mountains around Dilling (Fig. 2). As outlined by Rognon (1980), local morphologic or geologic parameters control in a large extent the local climate. In the case of the studied area of Kordofan, the orographic effect played by the Nuba Mountains may have fixed and concentrated the seasonal clouds and moisture of the ITCZ, enhancing precipitations and explaining the predominance of fluvial deposits in the southern areas, even during arid phases. The elevated central part of the study area (Fig. 2), may have still received rains from the clouds fixed by the nearby Nuba Mountains, thus explaining the presence of swamps not fed by rivers. Conversely, the northern areas located far from the Nuba Mountains were more affected by aeolian processes even during humid phases and received mainly sandy deposits, which may have accentuated the effects of aridity (Rognon, 1980). Nevertheless, the orographic effect played by inselbergs around Sodari (Fig. 2) may have favoured rains and the formation of the paleo-lakes around Sodari and El Ga'a (Fig. 1B). These geographic peculiarities, may account for the strong sedimentary and climatic gradient observed in the studied area, both during the Holocene and nowadays, and illustrates its location at the transition between the tropical and Saharan domains.

4. Summary

Our study of the Quaternary deposits of part of the Kordofan region led to some relevant results.

1. The surficial sediments of Kordofan are mostly latest Pleistocene to Holocene in age, if one omits the large NNE-SSW-trending dunes that marks the landscape in the northern part of the study area, which remain to be dated.
2. These deposits reveal a contrasting climatic evolution, which can be summed up as follows.
   - Between > 13 and 10.5 kyr BP, an arid period is marked by the deposition of well-sorted aeolian sands in most of the area.
   - From 10.5 to 6.5 kyr BP, a humid period, known as the African Humid period, is marked by (1) the local deposition of palustrine (central area) or lacustrine carbonates (northern area), which allowed the settlement of human populations, (2) the pedogenesis of the previously deposited sands in all areas, leading to mottling and development of calcareous concretions, and (3) a fluvial activity that probably removed most of the aeolian sands in the southern areas with contrasted topography (Dilling).
   - From 6.5 to ≈3.3 kyr BP, a progressive drying of the climatic conditions is recorded by the disappearance of palustrine or lacustrine deposits, and by the evolution from aquatic to terrestrial gastropod fauna, and from tropical to arid pollen assemblages.
   - Between 3.3 and 1.1 kyr BP, the whole area recorded either a sedimentary gap, or erosions, interpreted as due to a strong aeolian activity.
   - From 1.1 kyr BP to Present, deposition of aeolian sand resumed, which underwent partial pedogenesis and fluvial re-deposition in the southern areas.
3. This evolution also highlights a marked climatic contrast between the northern areas, dominated by aeolian processes related to mainly arid climatic conditions, and the southern areas, where fluvial processes were important, traducing a more humid climate during the studied period. This difference may be attributed to the orographic effect played by the nearby Nuba Mountains, and illustrates the location of the Kordofan Province in the Sahelian belt, intermediate between the Saharan desert and the tropical rain belt.
4. This sedimentary and climatic evolution of the Kordofan region is consistent with the evolution recorded in the neighboring areas. The identification of a period of strong wind activity and erosion (≈3.3 to 1.1 kyr BP) in Kordofan, which seems to correspond to an hyper arid period in Northeastern Africa, may have had significant consequences on the evolution of local human civilizations.

Acknowledgement

This study has been carried out in the framework of a PhD scholarship received by A. Dawelbeit from the Sudanese Government. Field trips and analyses have been financed by the French-Sudanese collaborative projects “Napata” n° 38408UF and 38730 A, by the ISTerre laboratory, and the IRD institution. We thank the French Embassy in Khartoum and the Sudanese Ministry of Higher Education and Scientific Research of Sudan for their helpful support in Sudan during this work. Special acknowledgements are due to D. Vandamme (Ghent, Belgium), C. Griggo (Chambéry, France), S. Ahmed and M.A. Howeida (Khartoum, Sudan), V. Magnin, N. Findling, M. Lanson, B. Lançon and C. Chauvel (Grenoble, France) for their invaluable assistance in the sample determinations and laboratory analyses. We warmly thank M.A.J. Williams and an anonymous reviewer for their useful and inspiring comments, which contributed to the improvement of this work.

Appendix A. Supplementary data

Supplementary data to this article can be found online at https://

doi.org/10.1016/j.jafrearsci.2019.103605.

References

Abell, P.I., Hoelzmann, P., 2000. Holocene palaeoclimates in northwestern Sudan: stable isotope studies on molluscs. Glob. Planet. Chang. 26, 1–12.
Alonso-Zarza, A.M., 2003. Palaeoenvironmental significance of palustrine carbonates and calcretes in the geological record. Earth Sci. Rev. 60, 261–298.
Alonso-Zarza, A.M., Genise, J.F., Verde, M., 2011. Sedimentology, diagenesis and ichnology of Cretaceous and Palaeogene calcretes and palustrine carbonates from Uruguay. Sediment. Geol. 236, 45–61.
Arakel, A.V., 1996. Quaternary vadose calcretes revisited. J. Aust. Geol. Geophys. 16, 223–229.
Barrows, T.T., Williams, M.A.J., Mills, S.C., Duller, G.A., Fifield, L.K., Habeerlah, D., TIms, S.G., Williams, F.M., 2014. A White Nile megalake during the last interglacial period. Geology 42, 163–166.
Bastian, L., Revel, M., Bayon, G., Dufour, A., Vigier, N., 2017. Abrupt response of chemical weathering to Late Quaternary hydroclimate changes in northeast Africa. Sci. Rep. 7, 44231. https://doi.org/10.1038/srep44231.
Blanchet, C.L., Tjallingii, R., Frank, M., Lorensen, J., Reitz, A., Brown, K., Feseker, T., Brückmann, W., 2013. High- and low-latitude forcing of the Nile River regime during the Holocene inferred from laminated sediments of the Nile deep-sea fan. Earth Planet. Sci. Lett. 364, 98–110.
Boggs, S., 2006. Principles of Sedimentology and Stratigraphy, fourth ed. Prentice-Hall, New Jersey, pp. 662.
Bristow, C.S., Armitage, S.J., 2016. Dune ages in the sand deserts of the southern Sahara and Sahel. Quat. Int. 410, 46–57.
Bubenzer, O., Besler, H., Hilgers, A., 2007. Filling the gap: OSL data expanding ^{14}C chronologies of Late Quaternary environmental changes in the Libyan Desert. Quat. Int. 175, 41–52.
Castaneda, I.S., Schouten, S., Pätzold, J., Lucassen, F., Kasemann, S., Kuhlmann, H., Schefuß, E., 2016. Hydroclimate variability in the Nile river basin during the past 28,000 years. Earth Planet. Sci. Lett. 438, 47–56.
Chen, X.Y., Lintern, M.J., Roach, I.C., 2002. Calcrete Characteristics, Distribution and Use in Mineral Exploration. Cooperative Research Centre for Landscape Environments and Mineral Exploration, Perth, Western Australia, pp. 160.
Ciolkosz, E.J., Dobos, R.R., 1990. Color and mottling in Pennsylvania soil. Agronomy series 108, 20. Pennsylvania state univ. https://ecosystems.psu.edu/research/pdf/as108.pdf.
Cole, J.M., Goldstein, S.L., deMenocal, P.B., Hemming, S.R., Grousset, F.E., 2009. Contrasting compositions of saharan dust in the eastern Atlantic ocean during the last deglaciation and African humid period. Earth Planet. Sci. Lett. 278, 257–266.
Collins, J.A., Gvin, A., Mulitza, S., Heslop, D., Zabel, M., Hartmann, J., Röhl, U., Wefer, G., 2013. Abrupt shifts of the sahara–sahel boundary during heinrich stadials. Clim. Past 9, 1181–1191.
Collins, J.A., Prange, M., Caley, T., Gimeno, L., Beckmann, B., Mulitza, S., Skonieczny, C., Roche, D., Schefuß, E., 2017. Rapid termination of the African Humid Period triggered by northern high-latitude cooling. Nature 8 (1372), 1–11. https://doi.org/10.1038/s41467-017-01454-y.
Collinson, J.D., 1986. Deserts. In: Reading, H.G. (Ed.), Sedimentary Environments and Facies. Blackwell, Oxford, pp. 95–112.
Costa, K., Russel, J., Konecky, B., Lamb, H., 2014. Isotopic reconstruction of the African humid period and Congo air boundary migration at lake tana, Ethiopia. Quat. Sci. Rev. 83, 58–67.
Dal Sasso, G., Zerboni, A., Maritan, L., Angelini, I., Compostella, C., Usai, D., Artioli, G., 2018. Radiocarbon dating reveals the timing of formation and development of pedogenic calcium carbonate concretions in Central Sudan during the Holocene. Geochem. Cosmochim. Acta 238, 16–35.
Dawelbeit, A., 2018. Late Quaternary Sedimentary and Paleoclimatic Evolution of Kordofan, Sudan. PhD Thesis. Univ. Grenoble Alpes, pp. 185. https://www.theses.fr/2018GREAU022.
deMenocal, P., Ortiz, J., Guilderson, T., Adkins, J., Sarnthein, M., Baker, L., Yarusinska, M., 2000. Abrupt onset and termination of the African Humid Period: rapid climate responses to gradual insolation forcing. Quat. Sci. Rev. 19, 347–361.
Drake, N.A., Bristow, C.S., 2006. Shorelines in the Sahara: geomorphological evidence for an enhanced monsoon from paleolake Megachad. Holocene 16, 901–911.
Drake, N.A., Blench, R.M., Armitage, S.J., Bristow, C.S., White, K.H., 2011. Ancient watercourses and biogeography of the Sahara explain the peopling of the desert. Proc. Natl. Acad. Sci. 108, 458–462.
Durand, M., Bourquin, S., 2013. Criteria for identification of ventifacts in the geological record: a review and new insights. Compt. Rendus Geosci. 345, 111–125.
Edmond, J.M., 1942. The distribution of the kordofan sands “Anglo-Egyptian Sudan”. Geol. Mag. 79, 18–30.
El Shafie, A.A.I., Zeinelabdein, K.A.E., Eisawi, A.A.M., 2011. Paleoclimatic evolution of central Sudan during the late miocene to Pleistocene. Arabian. J. Geosci. https://doi.org/10.1007/s12517-011-0435-z.
Foerster, V., Junginger, A., Langkamp, O., Gebru, T., Asrat, A., Umer, M., Lamb, H.F., Wennrich, V., Rethemeyer, J., Nowaczyk, N., Trauth, M.H., Schaebitz, F., 2012. Climatic change recorded in the sediments of the Chew Bahir basin, southern Ethiopia, during the last 45,000 years. Quat. Int. 274, 25–37.
Freytet, P., Plaziat, J., Verrecchia, E.P., 1997. A classification of rhizogenic (root-formed) calcretes, with examples from the Upper Jurassic-Lower Cretaceous of Spain and Upper Cretaceous of southern France – Discussion. Sediment. Geol. 110, 299–303.
Freytet, P., Verrecchia, E.P., 2002. Lacustrine and palustrine carbonate petrography: an overview. J. Paleolimnol. 27, 221–237.
Gasse, F., 2000. Hydrological changes in the African tropics since the last glacial maximum. Quat. Sci. Rev. 19, 189–211.
Gasse, F., Chalié, F., Vincens, A., Williams, M.A.J., Williamson, D., 2008. Climatic patterns in equatorial and southern Africa from 30,000 to 10,000 years ago reconstructed from terrestrial and near-shore proxy data. Quat. Sci. Rev. 27, 2316–2340.
Gatto, M.C., Zerboni, A., 2015. Holocene supra-regional environmental changes as trigger for major socio-cultural processes in Northeastern Africa and the Sahara. Afr. Archaeol. Rev. 32, 301–333.
Gierz, P., Werner, M., Lohmann, G., 2017. Simulating climate and stable water isotopes during the Last Interglacial using a coupled climate-isotope model. J. Adv. Model. Earth Syst. 9, 2027–2045. https://doi.org/10.1002/2017MS001056.
Glennie, K.W., 1987. Desert sedimentary environments, present and past – a summary. Sediment. Geol. 50, 135–165.
Gunn, R.H., 1982. The plains of the central and southern Sudan. In: Williams, M.A.J., Adamson, D.A. (Eds.), A Land between Two Niles: Quaternary Geology and Biology of the Central Sudan. A.A. Balkema, Rotterdam, pp. 81–109.
Haaland, R., 1992. Fish, pots and grain: early and Mid-Holocene adaptations in the Central Sudan. Afr. Archeol. Rev. 10, 43–64.
Hamann, Y., Ehrmann, W., Gerhard Schmiedl, G., Kuhnt, T., 2009. Modern and late Quaternary clay mineral distribution in the area of the SE Mediterranean Sea. Quat. Res. 71, 453–464.
Haynes, C.V., 1982. Great sand sea and Selima sand sheet: geochronology of desertification. Science 217, 629–633.
Hewaidy, A., Elshahat, O.R., Kamal, S., 2018. Stratigraphy, facies analysis and depositional environments of the upper unit of Abu roash “E” member in the Abu gharadig field, western desert, Egypt. J. Afr. Earth Sci. 139, 26–37.
Hoelzmann, P., Gasse, F., Dupont, L.M., Salzmann, U., Staubwasser, M., Leuschner, D.C., Sirocko, F., 2004. Palaeoenvironmental changes in the arid and subarid belt (SAHARA-Sahel-Arabian Peninsula) from 150 kyr to Present. In: Battarbee, R.W. (Ed.), Past Climate Variability through Europe and Africa.
Hoelzmann, P., Schwalb, A., Roberts, N., Cooper, P., Burgess, A., 2010. Hydrological response of an east-Saharan palaeolake (NW Sudan) to early-Holocene climate. Holocene 20, 537–549.
Kröpelin, S., Soulié-Märche, I., 1991. Charophyte remains from Wadi howar as evidence for deep mid-holocene freshwater lakes in the eastern Sahara of northwest Sudan. Quat. Res. 36, 210–223.
Kröpelin, S., Verschuren, D., Lézine, A.-M., Eggermont, H., Cocquyt, C., Francus, P., Cazet, J.-P., Fagot, M., Rumes, B., Russell, J.M., Darius, F., Conley, D.J., Schuster, M., von Suchodoletz, H., Engstrom, D.R., 2008. Climate-driven ecosystem succession in the Sahara: the past 6000 years. Science 320, 765–768.
Kuper, R., Kröpelin, S., 2006. Climate-controlled Holocene occupation in the Sahara: motor of Africa's evolution. Science 313, 803–807.
Lancaster, N., Kocurek, G., Singhvi, A., Pandey, V., Deynoux, M., Ghienne, J.-F., Lô, K., 2002. Late Pleistocene and Holocene dune activity and wind regimes in the Western Sahara Desert of Mauritania. Geology 30, 991–994.
Lézine, A.-M., 2009. Timing of vegetation changes at the end of the Holocene Humid Period in desert areas at the northern edge of the Atlantic and Indian monsoon systems. C. R. Geoscience 341, 750–759.
Lézine, A.-M., Zheng, W., Braconnot, P., Krinner, G., 2011. A late Holocene pollen and climate record from Lake Yoa, northern Chad. Clim. Past 7, 2413–2444.
Lewis, S.L., Maslin, M.A., 2015. Defining the anthropocene. Nature 519, 171–180.
Manning, K., Timpson, A., 2014. The demographic response to Holocene climate change in the Sahara. Quat. Sci. Rev. 101, 28–35.
Mohammed-Ali, A.S., Khabir, A.M., 2003. The wavy line and the dotted wavy line pottery in the prehistory of the central nile and the sahara-sahel belt. Afr. Archaeol. Rev. 20, 25–58.
Nicholson, S., Flohn, H., 1980. African environmental and climatic changes and the general atmospheric circulation in late Pleistocene and Holocene. Clim. Change 2, 313–348.
Nicoll, K., 2004. Recent environmental change and prehistoric human activity in Egypt and Northern Sudan. Quat. Sci. Rev. 23, 561–580.
Pachur, H.J., Kröpelin, S., 1987. Wadi howar: paleoclimatic evidence from an extinct river system in the SouthEastern Sahara. Science 237, 298–300.
Pachur, H.J., Hoelzmann, P., 1991. Paleoclimatic implications of late quaternary lacustrine sediments in western Nubia, Sudan. Quat. Res. 36 257-216.
Revel, M., Ducassou, E., Grousset, F.E., Bernasconi, S.M., Migeon, S., Revillon, S., Mascle, J., Murat, A., Zaragosi, S., Bosch, D., 2010. 100,000 years African monsoon variability recorded in sediments of the Nile margin. Quat. Sci. Rev. 29, 1342–1362.
Revel, M., Ducassou, E., Skonieczny, C., Colin, C., Bastian, L., Bosch, D., Migeon, S., Mascle, J., 2015. 20,000 years of Nile River dynamics and environmental changes in the Nile catchment area as inferred from Nile upper continental slope Sediments. Quat. Sci. Rev. 130, 200–221.
Rodis, H.G., Hassan, A., Wahadan, L., 1968. Groundwater Geology of Kordofan Province-Sudan, Contribution to the Hydrology of Africa and Mediterranean Region. United State government printing office, Washington.
Rognon, P., 1980. Pluvial and arid phases in the Sahara: the role of non-climatic factors. Paleoecology of Africa 12, 45–62.
Ruxton, B.P., Berry, L., 1978. Clay plain and geomorphic history of the Central Sudan - a review. Catena 5, 251–283.
Sadig, A.M., 2010. The Neolithic of the Middle Nile Region. An Archeology of Central Sudan and Nubia. Fountain Publisher, Kampala, pp. 220.
Salih, A.A.M., Elagib, N.A., Tjernström, M., Zhang, Q., 2018. Characterization of the Sahelian-Sudan rainfall based on observations and regional climate models. Atmos. Res. 202, 205–218.
Salvatori, S., Usai, D., 2007. The Sudanese Neolithic Revisited. Cahier de Recherches de

l'Institut de Papyrologie et d'Egyptologie de Lille, pp. 323–333 2006-2007.
Salvatori, S., Usai, D., Zerboni, A., 2011. Mesolithic site formation and palaeoenvironment along the White Nile (Central Sudan). Afr. Archaeol. Rev. 28, 177–211.
Salvatori, S., Usai, D., Abdelrahman, M.F., Di Matteo, A., Iacumin, P., Linseele, V., Magzoub, M.K., 2014. Archaeology at el-khiday: new insight on the prehistory and history of Central Sudan. In: Anderson, J.R., Welsby, D.A. (Eds.), The Fourth Cataract and beyond. Proceed. 12th Internat. Conf. Nubian Studiespp. 243–257.
Schmidt, M.W.I., Torn, M.S., Abiven, S., Dittmar, T., Guggenberger, G., Janssens, I.A., Kleber, M., Kögel-Knaber, I., Lehmann, J., Manning, D.A.C., Nannipieri, P., Rasse, D.P., Weiner, S., Trumbore, S.E., 2011. Persistence of soil organic matter as an ecosystem property. Nature 478, 49–56. https://doi.org/10.1038/nature10386. 7367.
Schrank, E., 1994. Nonmarine Cretaceous palynology of northern Kordofan, Sudan, with notes on fossil Salviniales (water ferns). Geol. Rundsch. 83, 773–786.
Schüster, M., Roquin, C., Duringer, P., Brunet, M., Caugy, M., Fontugne, M., Taïsso Mackaye, H., Vignaud, P., Ghienne, J.-F., 2005. Holocene lake mega-Chad palaeoshorelines from space. Quat. Sci. Rev. 24, 1821–1827.
Schwarz, T., 1994. Ferricrete formation and relief inversion: an example from Central Sudan. Catena 21, 257–268.
Servant, M., 1970. Données stratigraphiques sur le Quaternaire supérieur et récent au Nord-Est du Lac Tchad. Cah. 1'ORSTOM. Sér. Géol. 2, 95–114.
Servant, M., Servant-Vildary, S., 1980. L'environnement quaternaire du Lac Tchad. In: Williams, M.A.J., Faure, H. (Eds.), The Sahara and the Nile. Balkema, Rotterdam, pp. 133–162.
Shanahan, T.M., McKlay, N.P., Hughen, K.A., Oberpeck, J.T., Otto-Bliesner, B., Heil, C.W., Scholz, C.A., Peck, J., 2015. The time-transgressive termination of the African humid period. Nat. Geosci. 8, 140–144.
Skonieczny, C., Paillou, P., Bory, A., Bayon, G., Biscara, L., Crosta, X., Eynaud, F., Malaizé, B., Revel, M., Aleman, N., Barusseau, J.-P., Vernet, R., Lopez, S., Grousset, F., 2015. African humid periods triggered the reactivation of a large river system in Western Sahara. Nature 6, 1–6. https://doi.org/10.1038/ncomms9751.
Stokes, S., Bailey, R.M., Fedoroff, N., O'Marah, K.E., 2004. Optical dating of aeolian dynamism on the West African Sahelian margin. Geomorphology 59, 281–291.
Stuiver, M., Reimer, P.J., Reimer, R.W., 2019. Calib 7.1. [WWW program] at. http://calib.org.
Szabo, B.I., Haynes Jr., C.V., Maxwell, T.A., 1995. Ages of Quaternary pluvial episodes determined by uranium-series and radiocarbon dating of lacustrine deposits of Eastern Sahara. Palaeogeogr. Palaeoclimatol. Palaeoecol. 113, 227–242.
Swezey, C., 2001. Eolian sediment responses to late Quaternary climate changes: temporal and spatial patterns in the Sahara. Palaeogeogr. Palaeoclimatol. Palaeoecol. 167, 119–155.
Tierney, J.E., Lewis, S.C., Cook, B.I., LeGrande, A.N., Schmidt, G.A., 2011. Model, proxy and isotopic perspectives on the east African humid period. Earth Planet. Sci. Lett. 307, 103–112.
Tierney, J.E., deMenocal, P.B., 2013. Abrupt shifts in horn of Africa hydroclimate since the last glacial Maximum. Science 342 (6160), 843–846. https://doi.org/10.1126/science.1240411.
Tierney, J.E., deMenocal, P.B., Zander, P.D., 2017. A climatic context for the out-of-Africa migration. Geology 45, 1023–1036.
Tóth, J.A., Lajtha, K., Kotroczó, Z., Krakomperger, Z., Caldwell, B., Bowden, R., Papp, M., 2007. The effect of climate change on soil Organic Matter decomposition. Acta Silvatica Lignaria Hung. 3, 75–85.
Tucker, M.E., Wright, V.P., 1990. Carbonate Sedimentology. Blackwell, Oxford, pp. 482.
Vail, J.R., 1978. Outline of the geology and mineral deposits of the Democratic Republic of Sudan and adjacent areas. Overseas Geol. Miner. Resour. 49, 68 (Institute of Geological Sciences, London).
Voss, C.I., Solima, S.M., 2014. The transboundary non-renewable Nubian aquifer system of Chad, Egypt, Libya and Sudan: classical groundwater questions and parsimonious hydrogeologic analysis and modeling. Hydrogeol. J. 22, 441–468.
Warren, A., 1970. Dune trends and their implications in the central Sudan. Z. Geomorphol. Neue Folge. Suppl. 10, 154–180.
Whiteman, A.J., 1971. The Geology of the Sudan Republic. Oxford University press, pp. 290.
Williams, M.A.J., 2009. Late Pleistocene and Holocene environments in the Nile basin. Glob. Planet. Chang. 69, 1–15.
Williams, M.A.J., 2014. Climate Change in Deserts (Past, Present and Future). Cambridge University Press, New York, pp. 629.
Williams, M.A.J., Adamson, D., Cock, B., McEvedy, R., 2000. Late quaternary environments in the white nile region, Sudan. Glob. Planet. Chang. 26, 305–316.
Williams, M.A.J., Talbot, M., Aharon, P., Salaam, Y.A., Williams, F., Brendeland, K.I., 2006. Abrupt return of the summer monsoon 15,000 years ago: new supporting evidence from the lower White Nile valley and Lake Albert. Quat. Sci. Rev. 25, 2651–2665.
Williams, M.A.J., Usai, D., Salvatori, S., Williams, F.M., Zerboni, A., Maritan, L., Linseele, V., 2015. Late Quaternary environments and prehistoric occupation in the lower White Nile valley, central Sudan. Quat. Sci. Rev. 130, 72–88.
Woodward, J.C., Macklin, M.G., Michael, D., Krom, D., Williams, M.A., 2007. The Nile: Evolution, Quaternary River Environments and Material Fluxes. John Wiley & Sons Ltd. Large Rivers: Geomorphology and Management.
Zerboni, A., Nicoll, K., 2019. Enhanced zoogeomorphological processes in North Africa in the human-impacted landscapes of the anthropocene. Geomorphology 331, 22–35.